

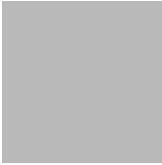
WIR SCHAFFEN WISSEN – HEUTE FÜR MORGEN



Cinthia Piamonteze:: Paul Scherrer Institute

X-Ray Absorption Spectroscopy

Cinthia.Piamonteze@PSI.ch



On A New Kind Of Rays

W.C. Röntgen, 1895

ON A NEW KIND OF RAYS.¹

(1) A DISCHARGE from a large induction coil is passed through a Hittorf's vacuum tube, or through a well-exhausted Crookes' or Lenard's tube. The tube is surrounded by a fairly close-fitting shield of black paper; it is then possible to see, in a completely darkened room, that paper covered on one side with barium platino-cyanide lights up with brilliant fluorescence when brought into the neighbourhood of the tube, whether the painted side or the other be turned towards the tube. The fluorescence is still visible at two metres distance. It is easy to show that the origin of the fluorescence lies within the vacuum tube.

(2) It is seen, therefore, that some agent is capable of penetrating black cardboard which is quite opaque to ultra-violet light, sunlight, or arc-light. It is therefore of interest to investigate how far other bodies can be penetrated by the same agent. It is readily shown that all bodies possess this same transparency, but in very varying degrees. For example, paper is very transparent; the fluorescent screen will light up when placed behind a book of a thousand pages; printer's ink offers no marked resistance. Similarly the fluorescence shows behind two packs of cards; a single card does not visibly diminish the brilliancy of the light. So, again, a single thickness of tinfoil hardly casts a shadow on the screen; several have to be superposed to produce a marked effect. Thick blocks of wood are still transparent. Boards of pine two or three centimetres thick absorb only very little. A piece of sheet aluminium, 15 mm. thick, still allowed the X-rays (as I will call the rays, for the sake of brevity) to pass, but greatly reduced the fluorescence. Glass plates of similar thickness behave similarly; lead glass is, however, much more opaque than glass free from lead. Ebonite several centimetres thick is transparent. If the hand be held before the fluorescent screen, the shadow shows the bones darkly, with only faint outlines of the surrounding tissues.



¹ By W. C. Röntgen. Translated by Arthur Stanton from the *Sitzungsberichte der Würzburger Physik-med. Gesellschaft*, 1895.

Typical questions for X-ray absorption



Typical questions for X-ray absorption

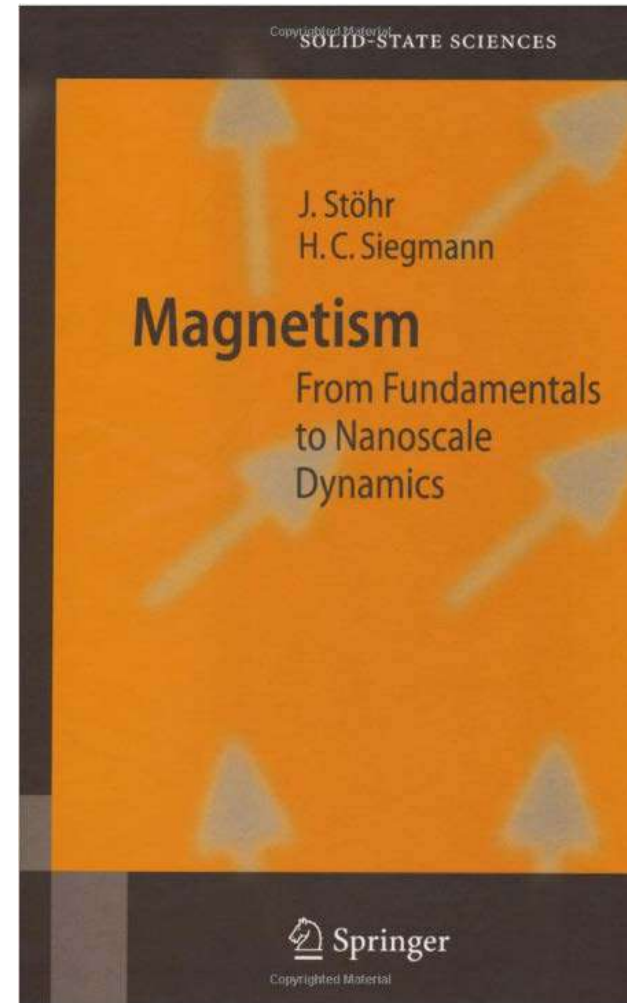
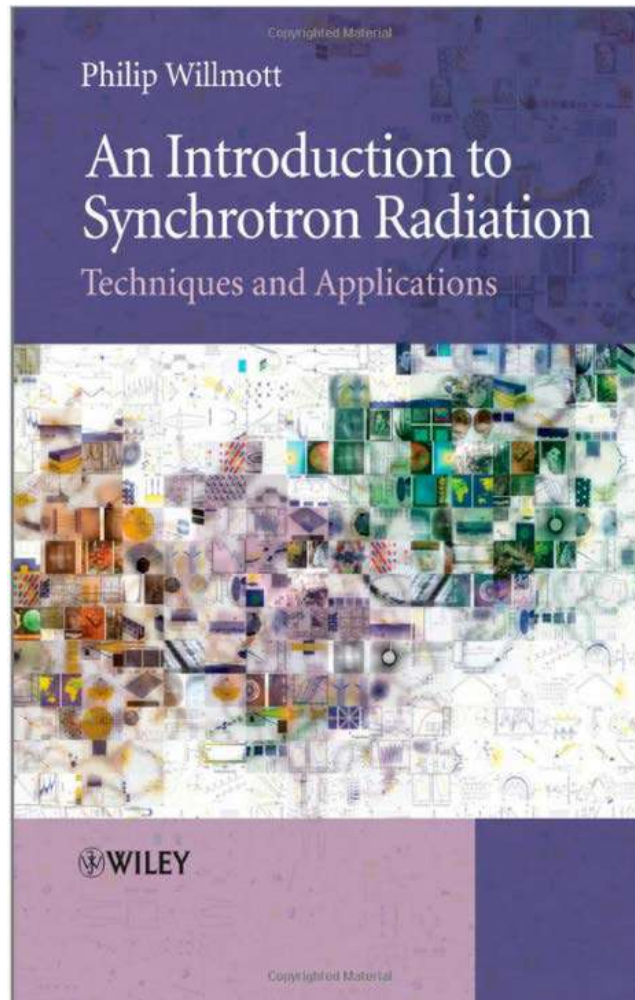


What is the valence state?


What is the orbital occupation?


What is the magnetic coupling?

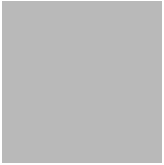
References



Outline of two lectures

- 
- A solid grey square is positioned to the left of the first bullet point.
- Lecture I:
 - X-ray absorption
 - Lecture II:
 - Polarized x-rays: (circular / linear) dichroism

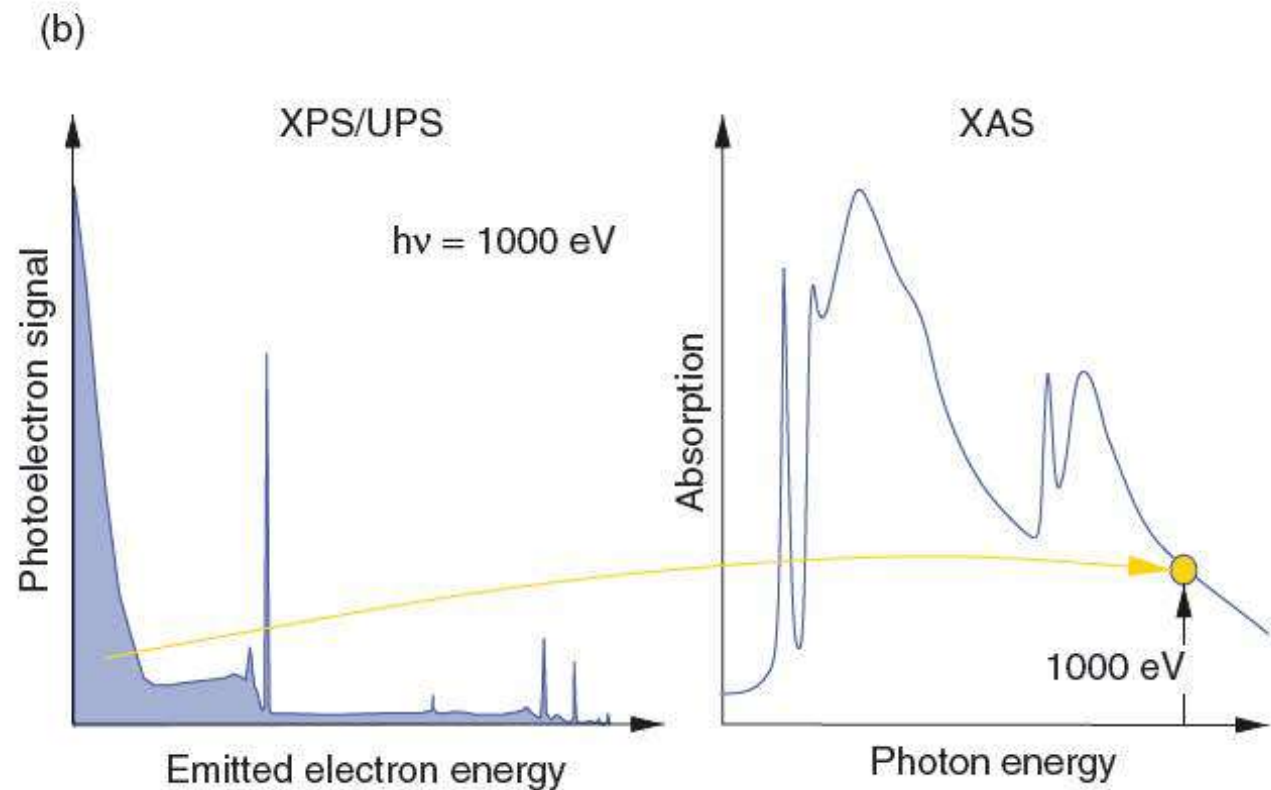
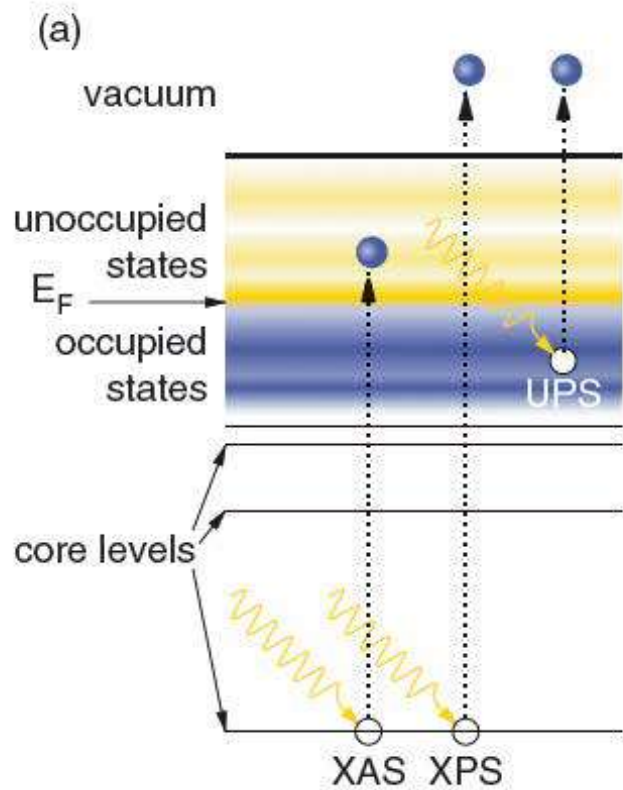
- 
- A solid grey square is positioned to the left of the first bullet point in the outline.
- General characteristics of synchrotron radiation
 - Description of x-ray absorption in general
 - Extended x-ray absorption fine structure (EXAFS)
 - Examples
 - X-ray absorption at L-edges of transition metals
 - Experimental setup
 - Detection methods
 - Examples



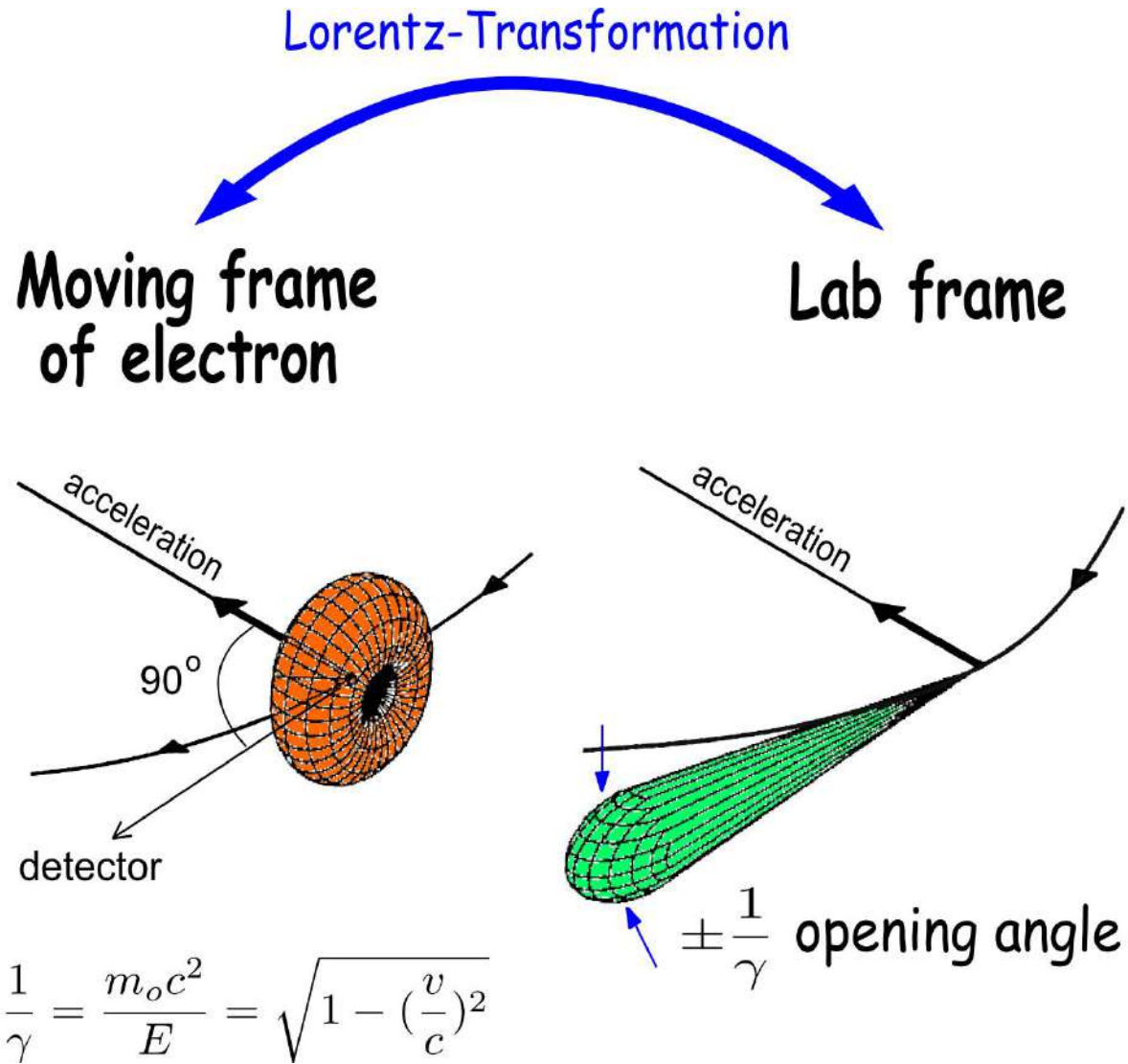
XPS vs XAS

X-ray absorption requires a tunable and intense x-ray source:

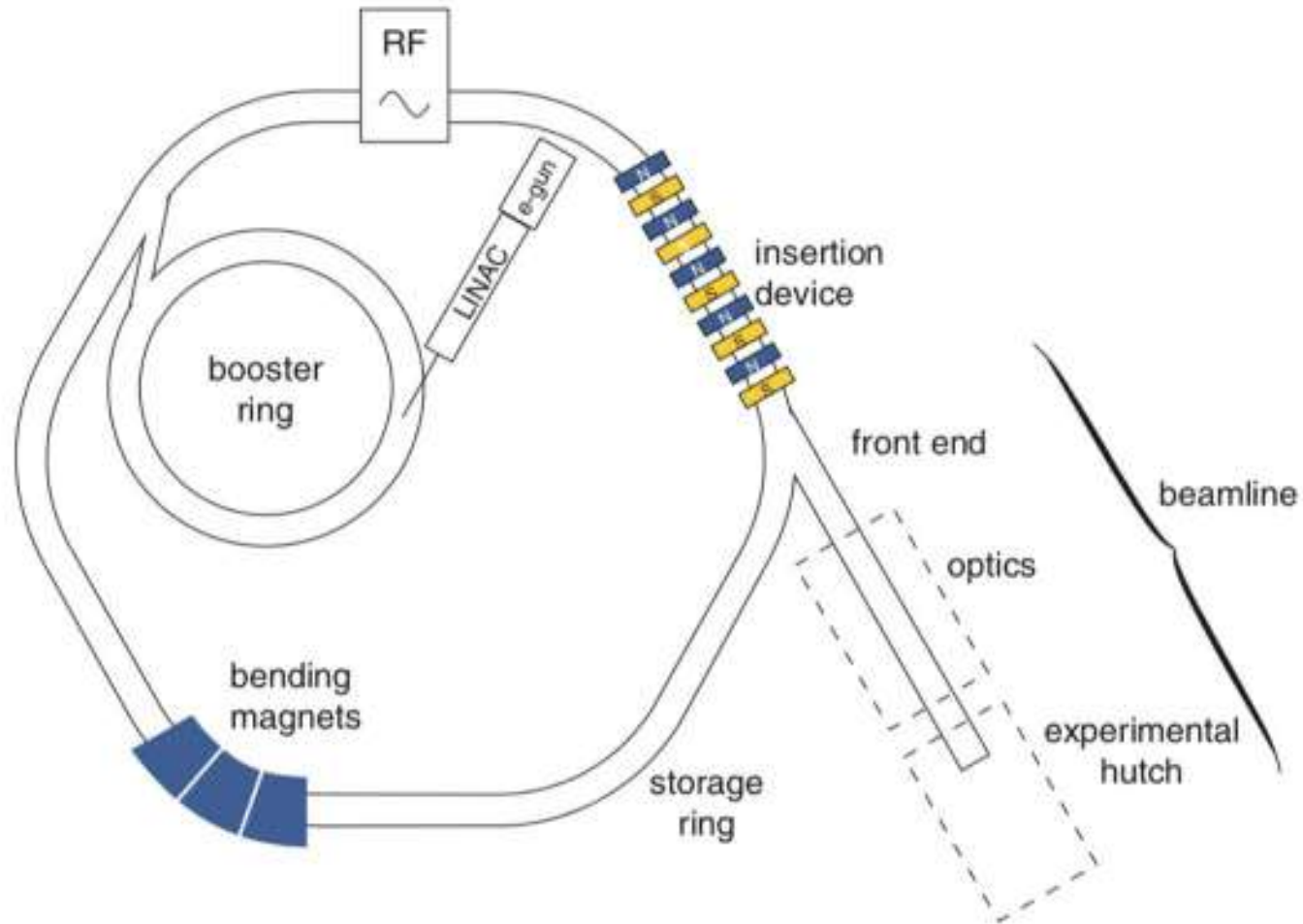
=> synchrotron sources: source of intense and polarized x-rays



Synchrotron radiation - divergence



Source – Synchrotron

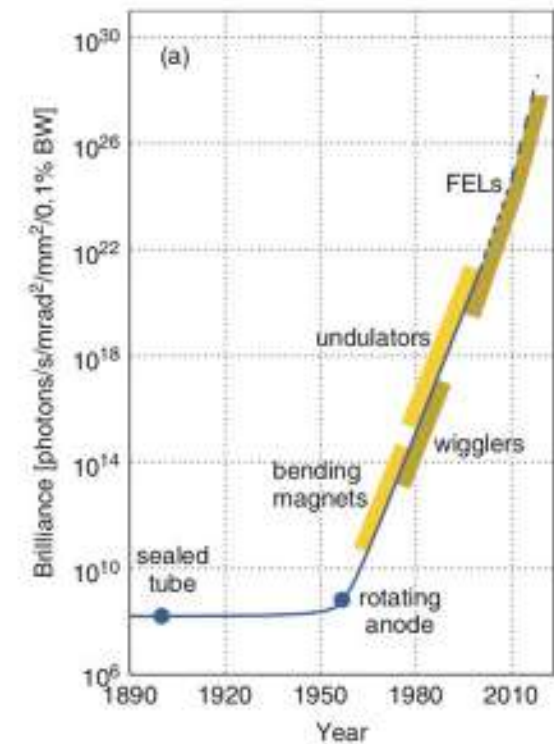




SLS storage ring – 330 magnets

Characteristics relevant to x-ray absorption

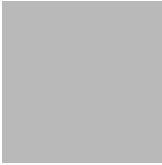
- High photon flux
- Small divergence => high brilliance
- Continuous in energy



Synchrotron Sources: Free Access

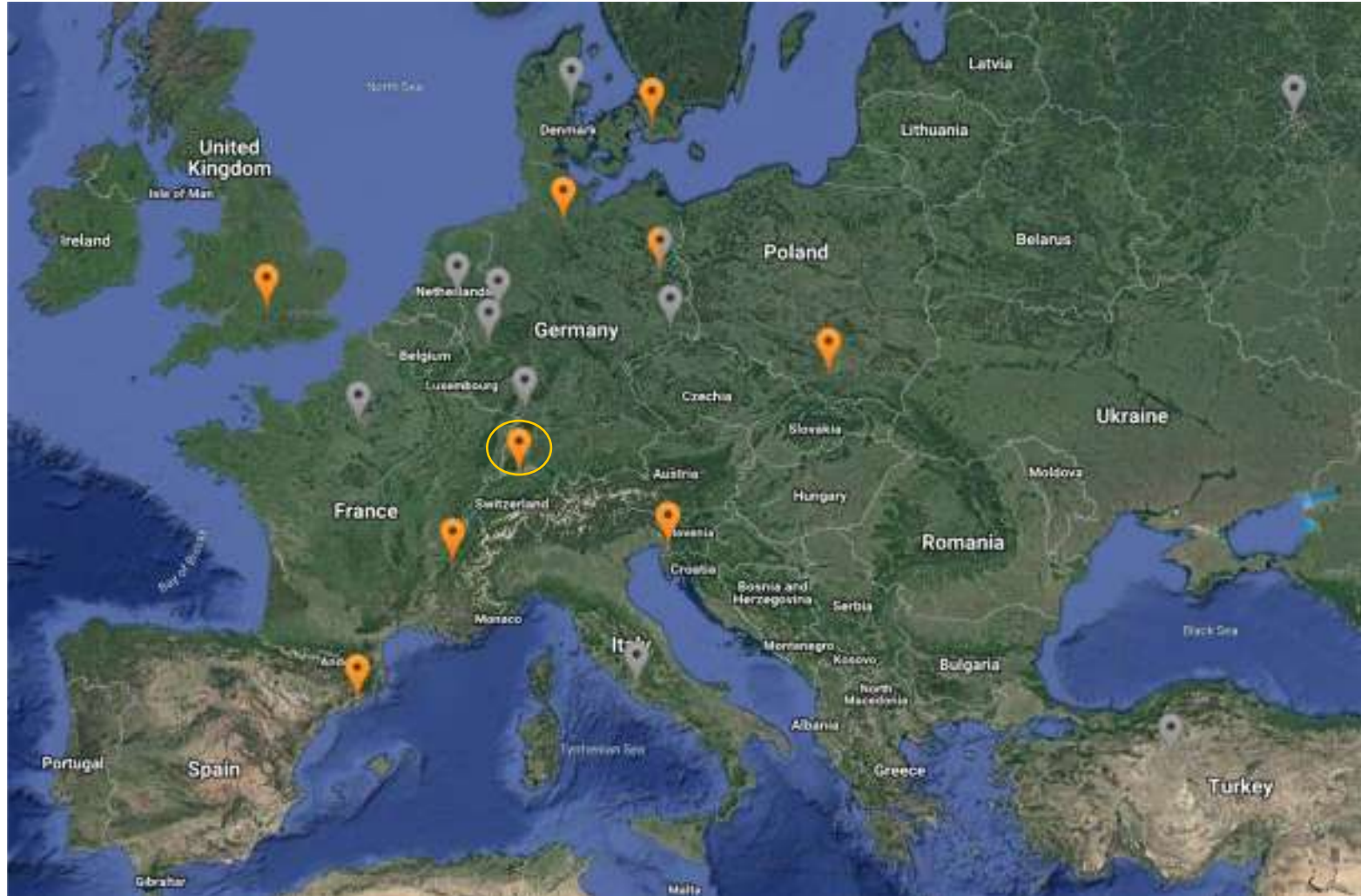
- Access by scientific merit through proposal submission
- Proposal submission deadlines for SLS: Sept. 15th ; March 15th
- Duo.PSI.ch

Synchrotron sources in the world



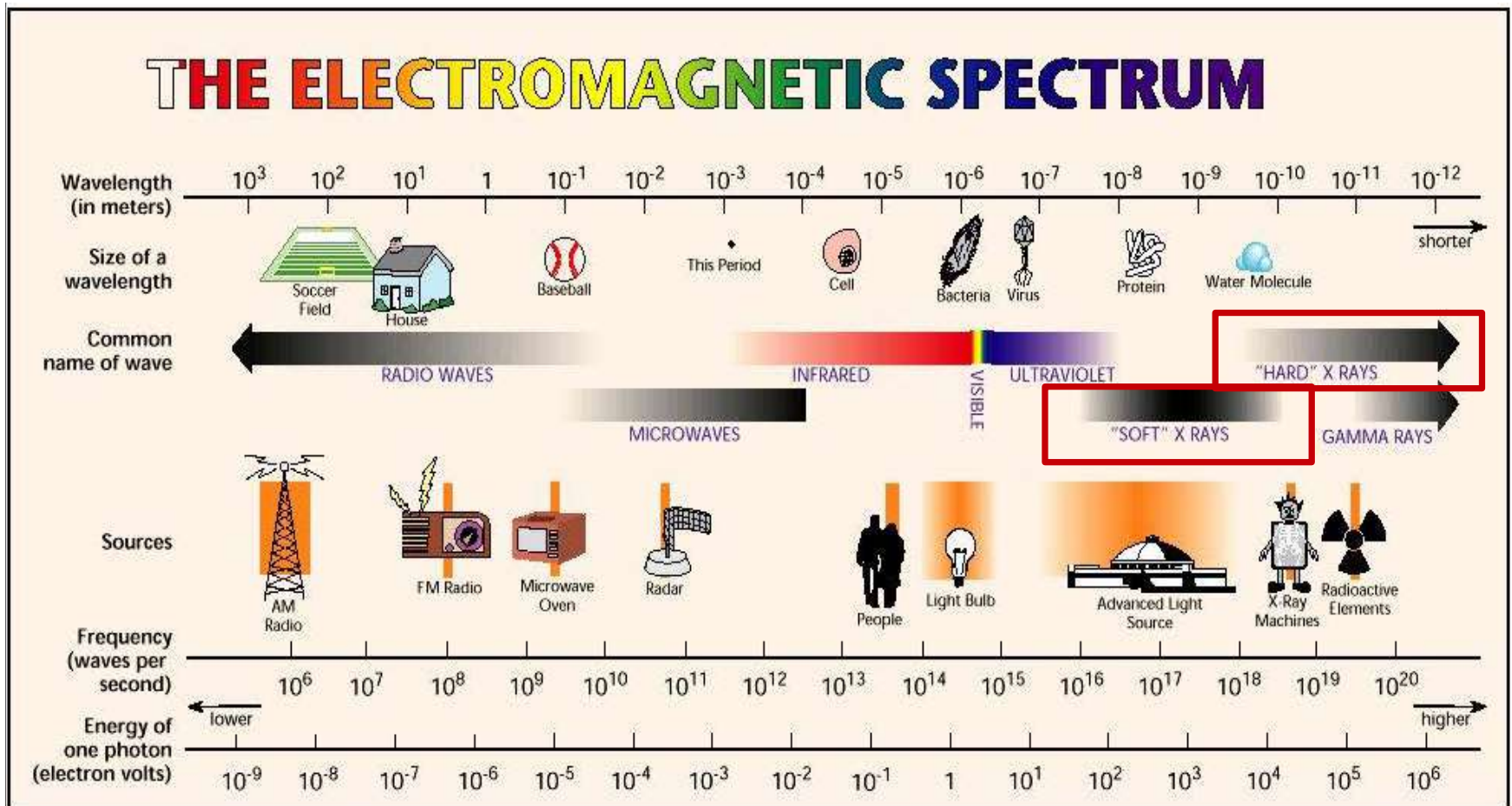
Source: lightsources.org

Synchrotron sources in Europe



Source: lightsources.org

THE ELECTROMAGNETIC SPECTRUM

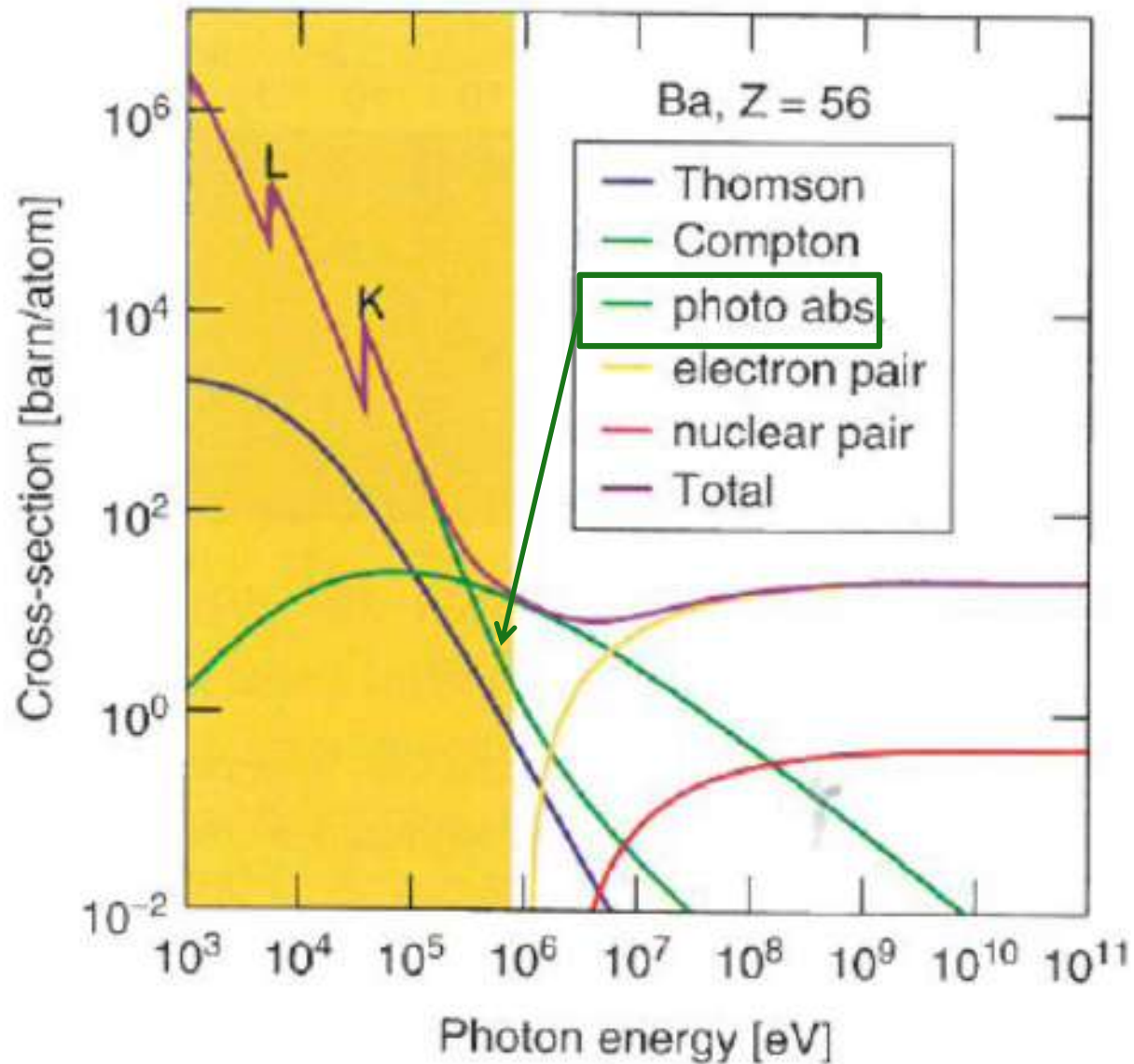


Courtesy of the Advanced Light Source, Berkeley Lab

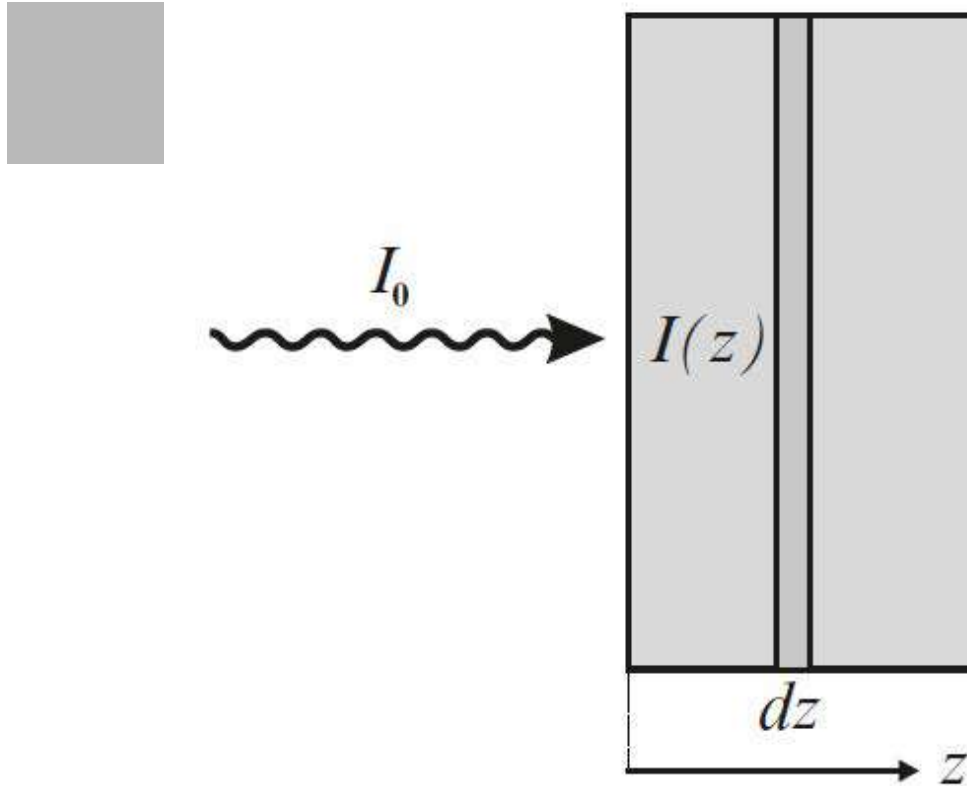
XBD 9510-06262.ILR

$$E = h\nu = hc/\lambda, \quad \lambda[\text{\AA}] = \frac{12.3984}{E[\text{keV}]}$$

Cross sections of photon interaction



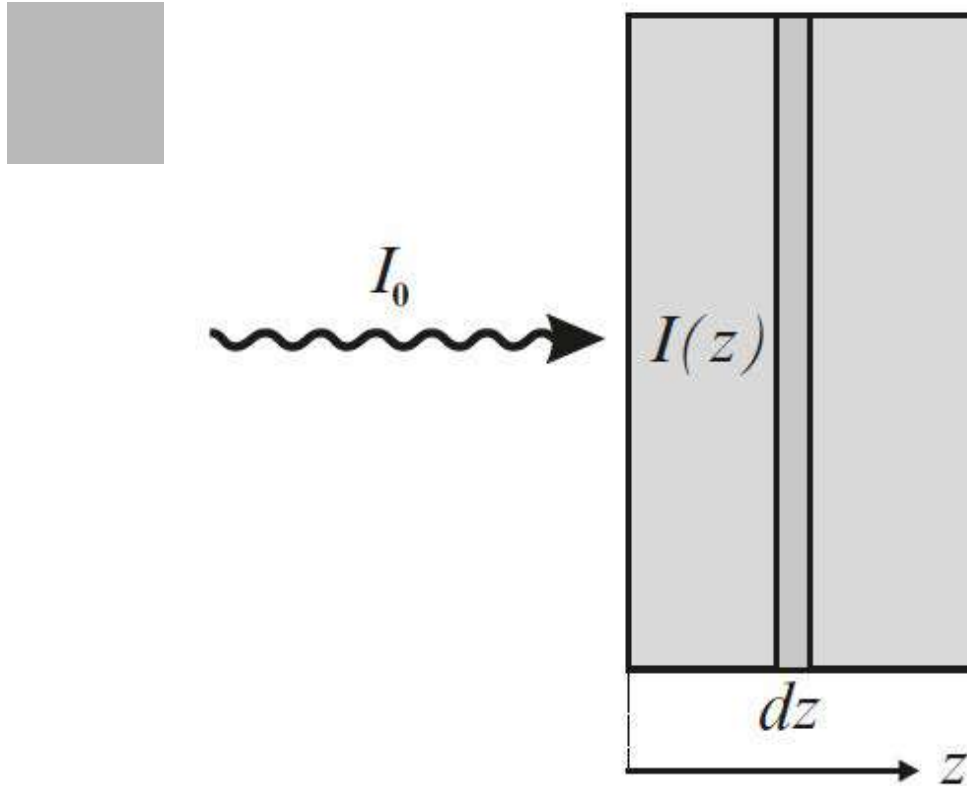
Linear x-ray absorption coefficient



The beam is attenuated by $\mu_x dz$ due to a sheet of thickness dz :

$$-dI(z) = I(z) \mu_x dz$$

Linear x-ray absorption coefficient



The beam is attenuated by $\mu_x dz$ due to a sheet of thickness dz :

$$-dI(z) = I(z) \mu_x dz$$

$$I(z) = I_0 e^{-\mu_x z}$$

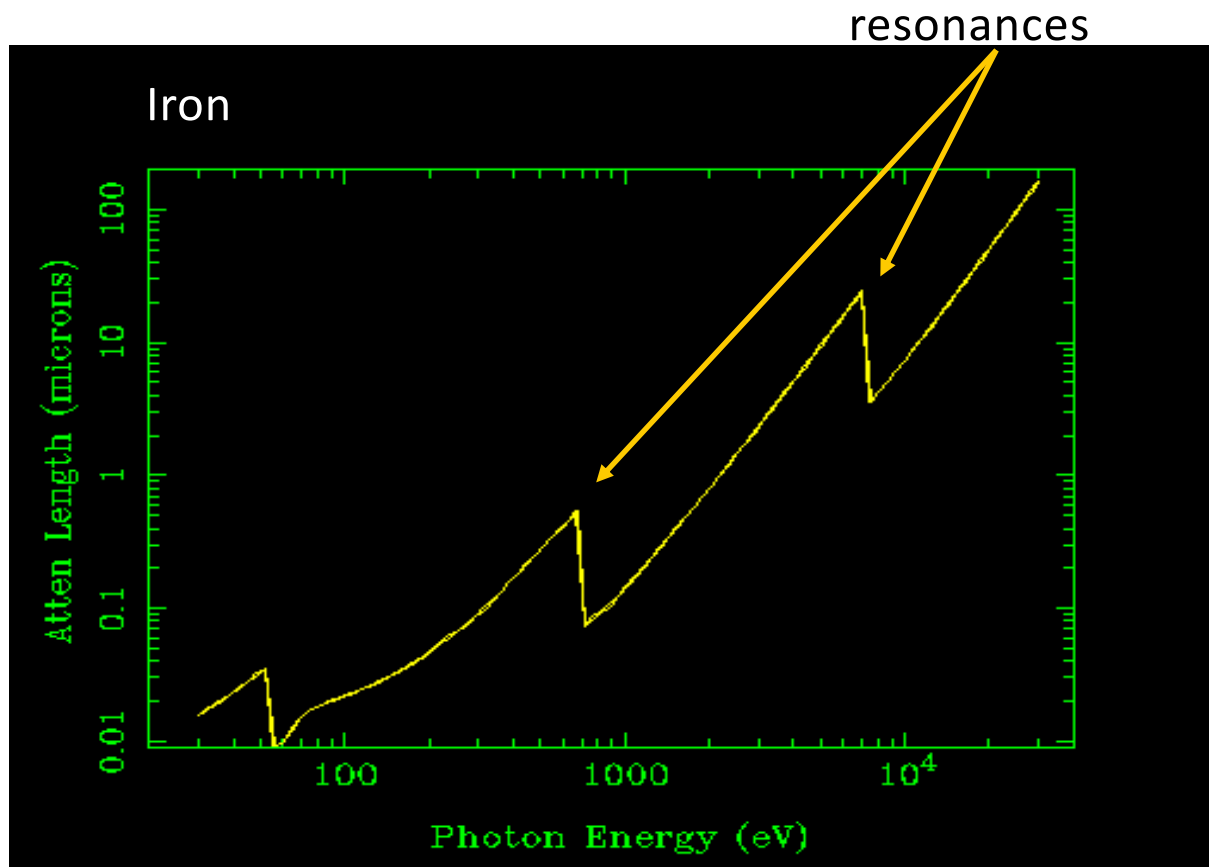
μ_x is the linear x-ray absorption coefficient

Unit: [1/distance]

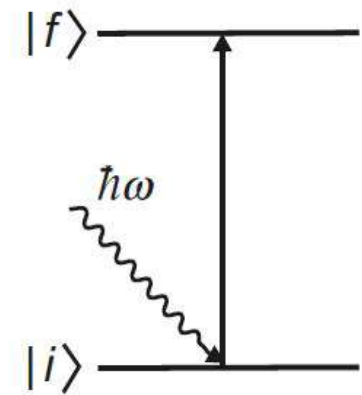
Attenuations length (λ_x)

$$I(z) = I_0 e^{-\mu_x z}$$

$$\lambda_x = 1/\mu_x$$



(a) X-Ray absorption



data from: http://henke.lbl.gov/optical_constants/

Refractive index, linear absorption coefficient, absorption cross section

$$\beta = \frac{\mu_x}{2k} = \frac{\rho_a}{2k} \sigma^{\text{abs}}$$

β : imaginary part of refractive index (dimensionless)

μ_x : linear absorption coefficient ([1/length])

$\lambda_x = 1 / \mu_x$ is the x-ray attenuation length:

k : $2\pi/\lambda$, where λ is the x-ray wavelength

ρ_a : atomic number density ([atoms/volume])

σ^{abs} : x-ray absorption cross section ([length²/atom])

Refractive index, linear absorption coefficient,
absorption cross section

$$\beta = \frac{\mu_x}{2k} = \frac{\rho_a}{2k} \sigma^{\text{abs}}$$

$$\sigma = \frac{T_{if}}{\Phi_0} .$$

T_{if} : transition probability per unit time

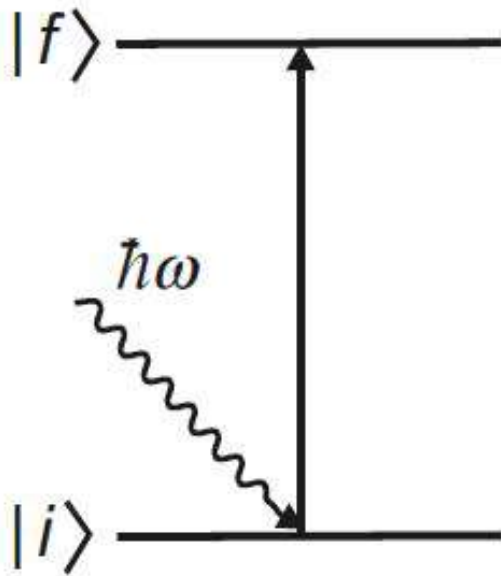
Φ_0 : incident photon flux

Transition probability per unit time

$$T_{if} = \frac{2\pi}{\hbar} |\langle f | \mathcal{H}_{int} | i \rangle|^2 \underbrace{\delta(\hbar\omega + \varepsilon_i - \varepsilon_f)}_{\text{energy conservation}} \underbrace{\rho(\varepsilon_f)}_{\text{density of final unoccupied states}}$$

energy conservation density of final unoccupied states

(a) X-Ray absorption



$$\mathcal{H}_e^{int} = \frac{e}{m_e} \mathbf{p} \cdot \mathbf{A}$$

electron momentum operator electric field from electromagnetic wave

Matrix element

$$T_{if} = \frac{2\pi}{\hbar} |\langle f | \mathcal{H}_{int} | i \rangle|^2 \delta(\hbar\omega + \varepsilon_i - \varepsilon_f) \rho(\varepsilon_f)$$

$$\mathcal{M} = \langle b | \mathbf{p} \cdot \boldsymbol{\epsilon} e^{i\mathbf{k} \cdot \mathbf{r}} | a \rangle$$

$$\mathcal{M} = \langle b | \mathbf{p} \cdot \boldsymbol{\epsilon} (1 + i\mathbf{k} \cdot \mathbf{r} + \dots) | a \rangle$$

$$\mathbf{k} \cdot \mathbf{r} = \frac{2\pi}{\lambda} \boldsymbol{\epsilon} \cdot \mathbf{r}$$

for soft x-rays $\lambda \sim 1\text{nm}$

2p core shell $r \sim 0.01\text{nm}$

$$\mathbf{k} \cdot \mathbf{r} \ll 1$$

Matrix element

$$T_{if} = \frac{2\pi}{\hbar} |\langle f | \mathcal{H}_{int} | i \rangle|^2 \delta(\hbar\omega + \varepsilon_i - \varepsilon_f) \rho(\varepsilon_f)$$

$$\mathcal{M} = \langle b | \mathbf{p} \cdot \boldsymbol{\epsilon} e^{i\mathbf{k} \cdot \mathbf{r}} | a \rangle$$

$$\mathcal{M} = \langle b | \mathbf{p} \cdot \boldsymbol{\epsilon} (1 + i\mathbf{k} \cdot \mathbf{r} + \dots) | a \rangle \simeq \langle b | \mathbf{p} \cdot \boldsymbol{\epsilon} | a \rangle = im_e \omega \langle b | \mathbf{r} \cdot \boldsymbol{\epsilon} | a \rangle$$



dipolar approximation

$$\mathbf{k} \cdot \mathbf{r} \ll 1$$

Dipolar approximation

dipolar approximation $k \cdot r \ll 1 \Rightarrow r \ll \frac{1}{k} = \frac{\lambda}{2\pi}$

assumes that the size of the absorbing atomic shell is small relative to x-ray wavelength

$$\mathcal{M} = \langle b | \mathbf{p} \cdot \boldsymbol{\epsilon} (1 + i\mathbf{k} \cdot \mathbf{r} + \dots) | a \rangle \simeq \langle b | \mathbf{p} \cdot \boldsymbol{\epsilon} | a \rangle = im_e \omega \langle b | \mathbf{r} \cdot \boldsymbol{\epsilon} | a \rangle$$

for soft x-rays $\lambda \sim 1\text{nm}$

2p core shell $r \sim 0.01\text{nm}$

$$\mathcal{M} = \langle b | \mathbf{p} \cdot \boldsymbol{\epsilon} (1 + i\mathbf{k} \cdot \mathbf{r} + \dots) | a \rangle \simeq \langle b | \mathbf{p} \cdot \boldsymbol{\epsilon} | a \rangle = im_e \omega \langle b | \mathbf{r} \cdot \boldsymbol{\epsilon} | a \rangle$$

\mathbf{r} : electric dipole operator

allows transition between orbitals such that:

$$\Delta l = \pm 1; \Delta s = 0$$

dipole selection rules

The dipole selection rules can be interpreted as follows:

- The x-ray has an angular momentum and therefore allows transition between states that change the angular momentum (l) by 1
- The x-ray has no spin moment and therefore it allows transition between state where the spin moment (s) does not change

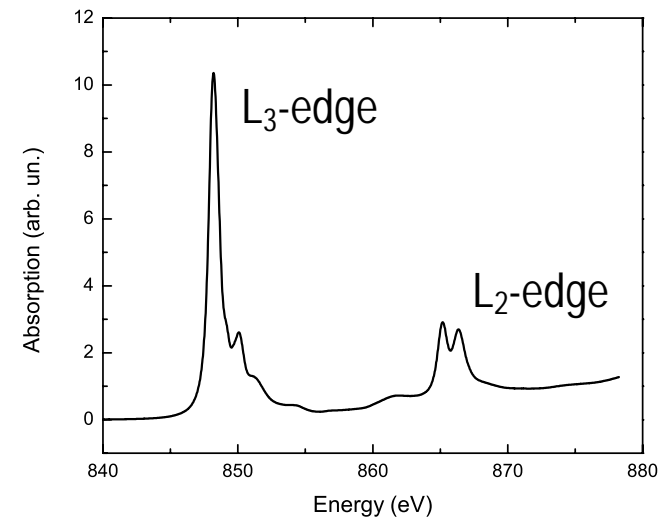
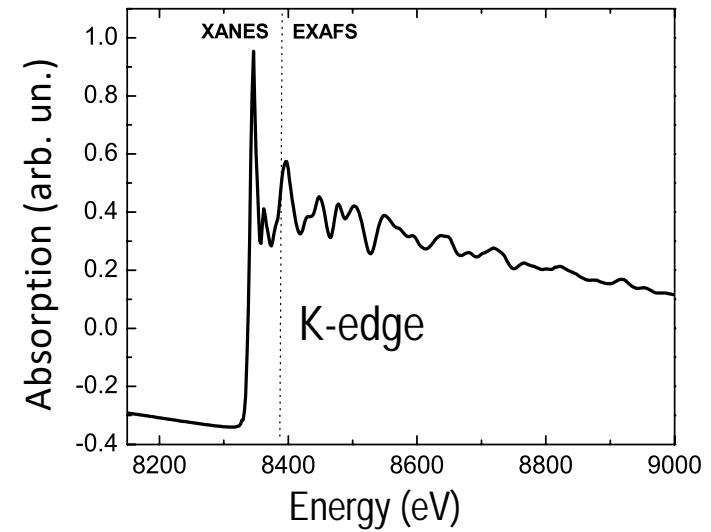
Dipole selection rules

$$\Delta l = \pm 1; \Delta s = 0$$

1s core state
transition

2p core state
transition

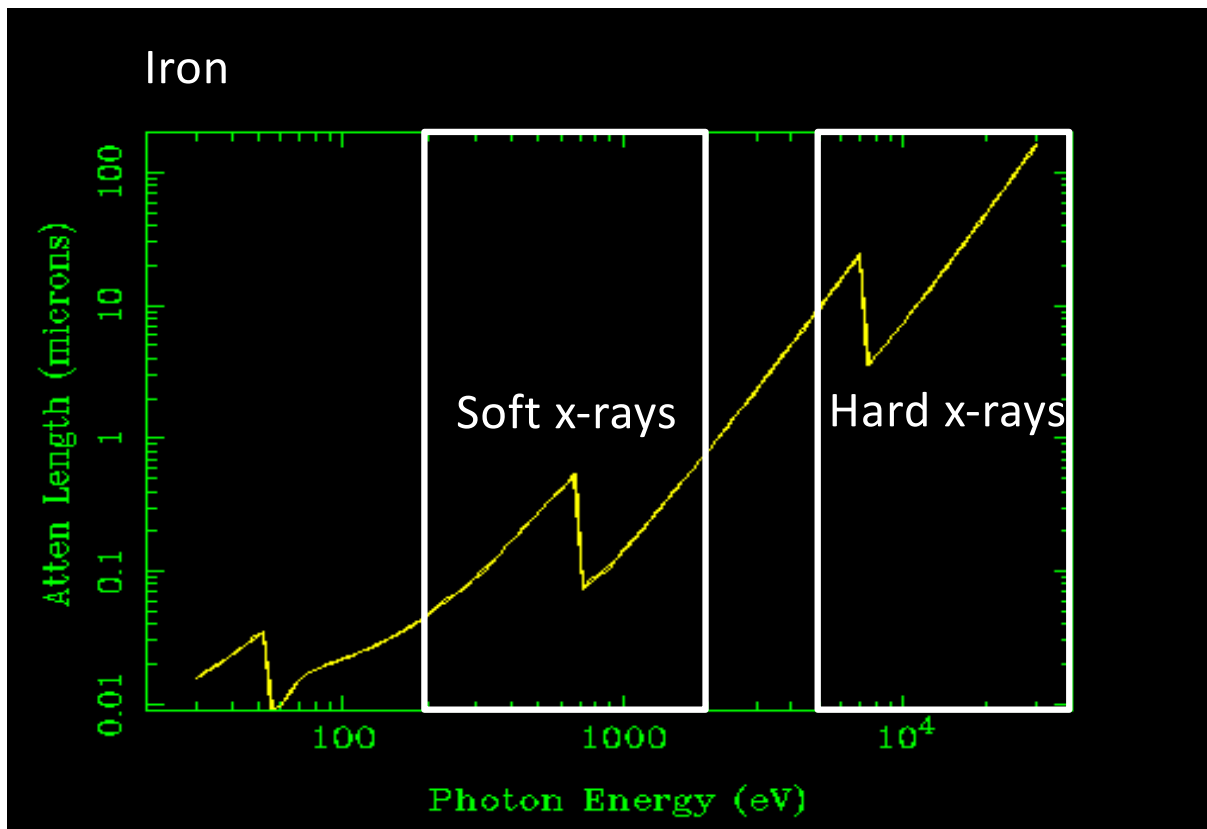
Ni absorption edges in NiO



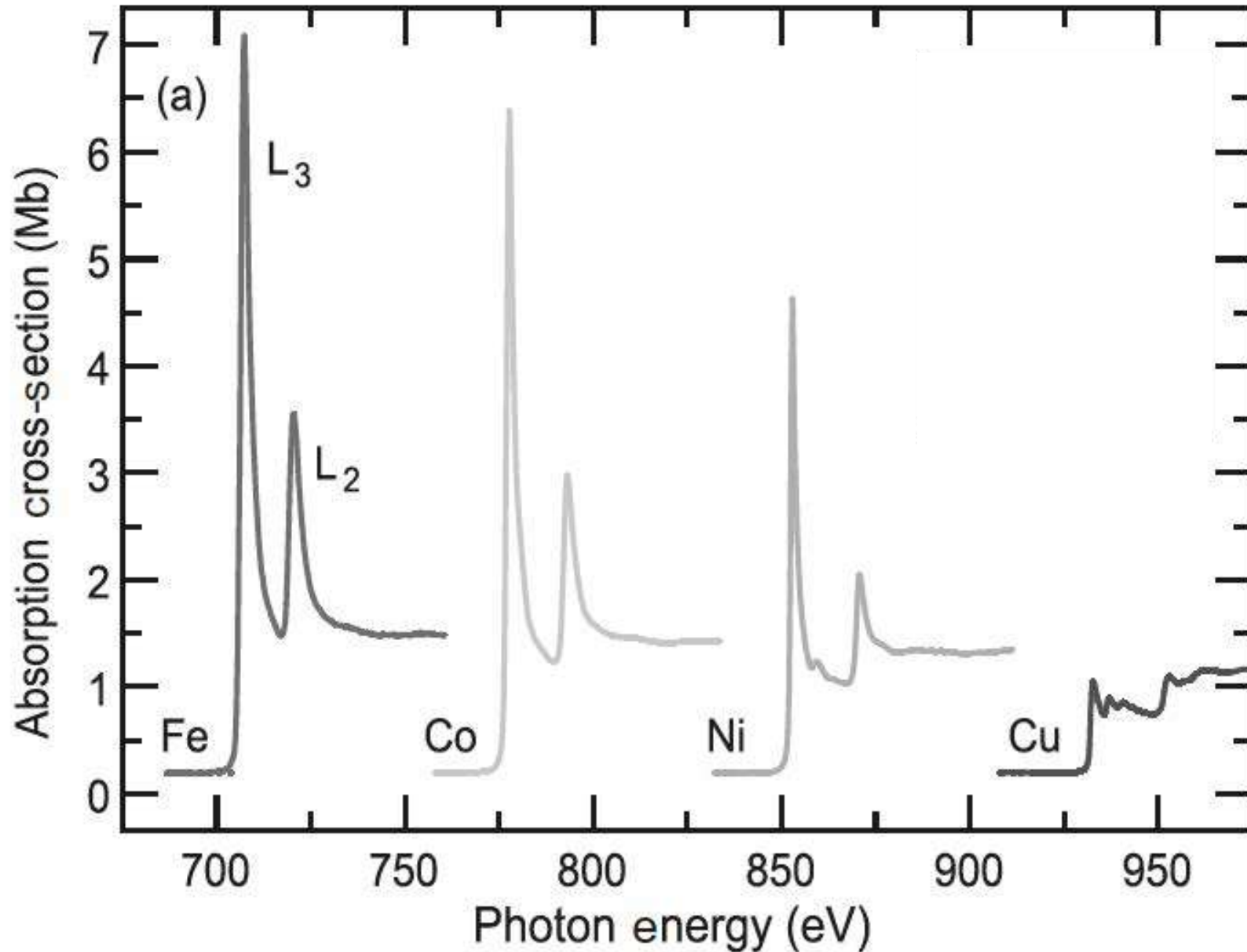
Tabulated attenuation lengths (λ_x)

$$I(z) = I_0 e^{-\mu_x z}$$

$$\lambda_x = 1/\mu_x$$



data from: http://henke.lbl.gov/optical_constants/



- X-ray absorption probes the density of unoccupied states
- XAS is element specific
- The strongest transition is through electric dipole

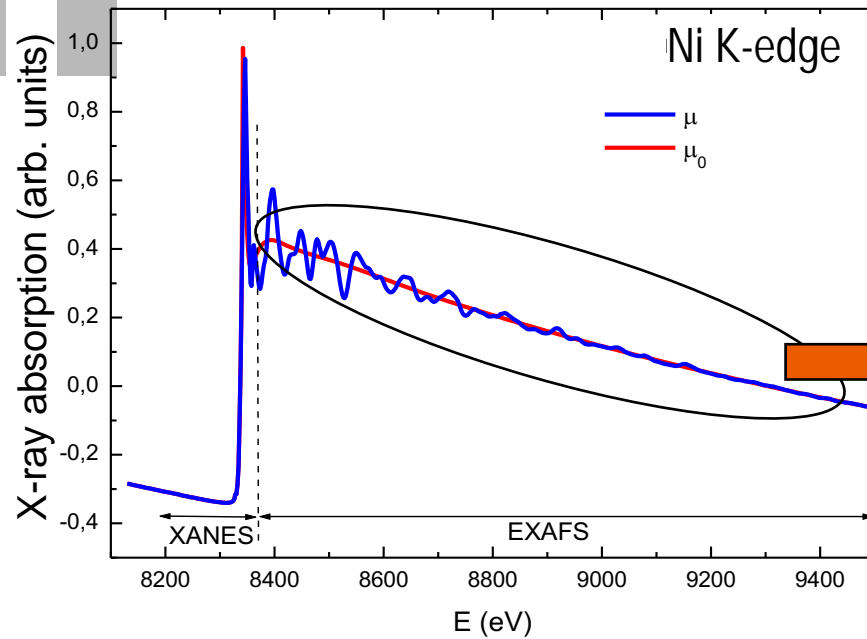
–dipole selection rules:

$$\Delta l = \pm 1; \Delta s = 0$$

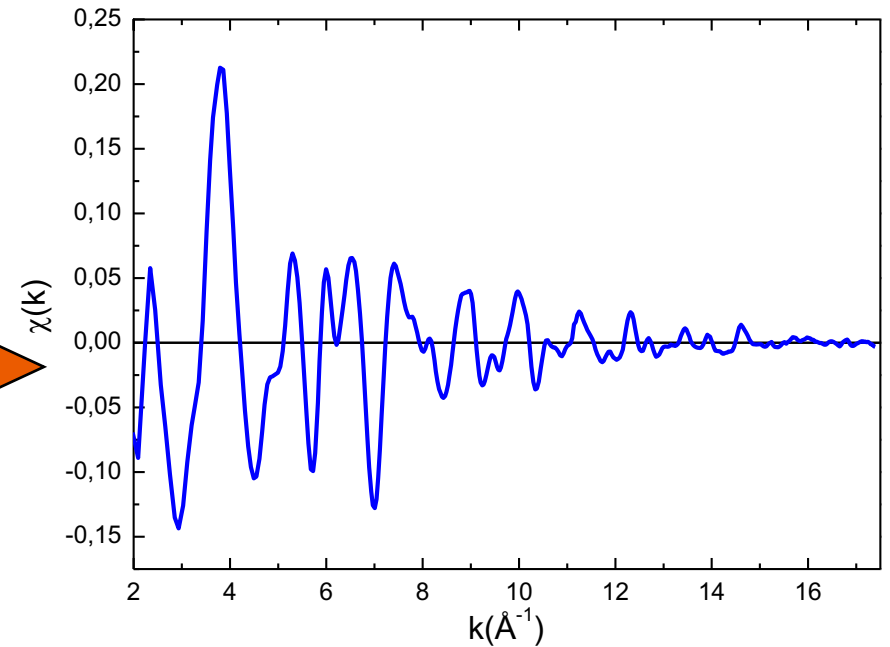


EXAFS

Extended X-ray Absorption Fine Structure



EXAFS signal

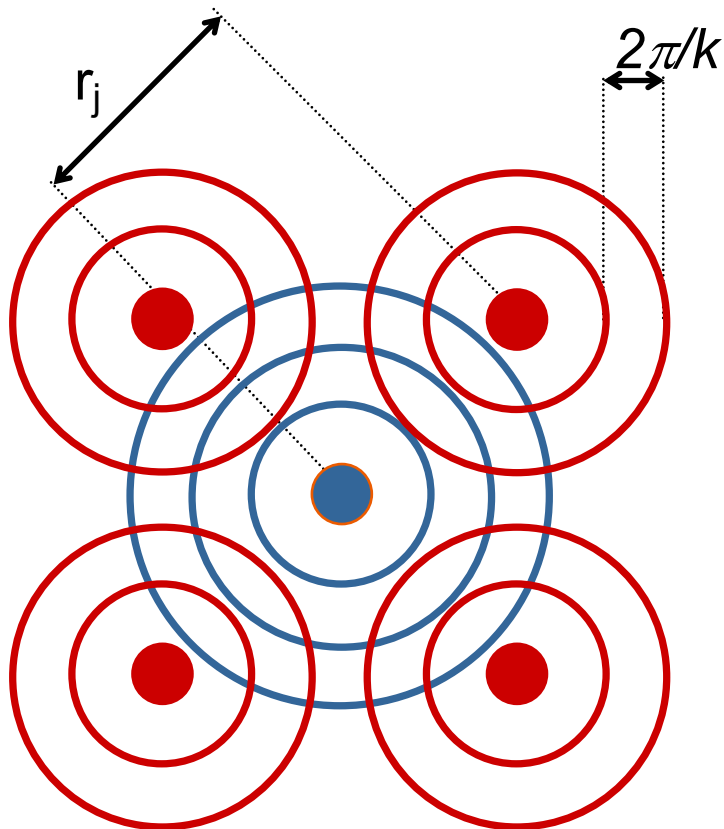


$$\chi(k) = \frac{\mu - \mu_0}{\mu_0}$$

$$\left\{ \begin{array}{l} \mu_0: \text{atomic absorption} \\ k = \sqrt{2m(E - E_0)} / \hbar \quad [1/\text{distance}] \end{array} \right.$$

EXAFS equation

$$\chi(k) = \sum_j \frac{N_j}{kr_j^2} F_j(k, \pi) \sin[2kr_j + \psi_j(k)] e^{-2\sigma_j^2 k^2} e^{-2r_j/\lambda_j(k)}$$



r_j : interatomic distance

N_j : number of neighbors

σ_j : Debye-Waller factor

F_j : back-scattering amplitude

ψ_j : phase shift

λ_j : electron mean free path

● Absorbing atom

● Scatterer

New Technique for Investigating Noncrystalline Structures: Fourier Analysis of the Extended X-Ray–Absorption Fine Structure*

Dale E. Sayers† and Edward A. Stern‡

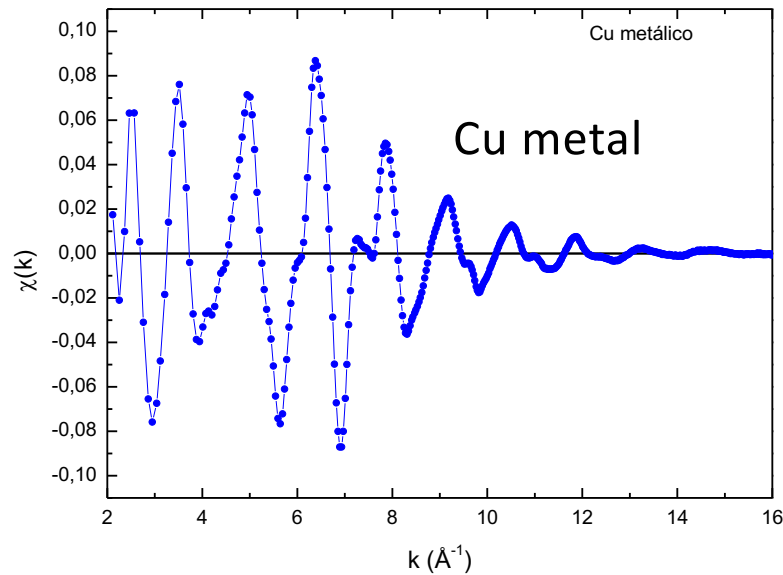
Department of Physics, University of Washington, Seattle, Washington 98105

and

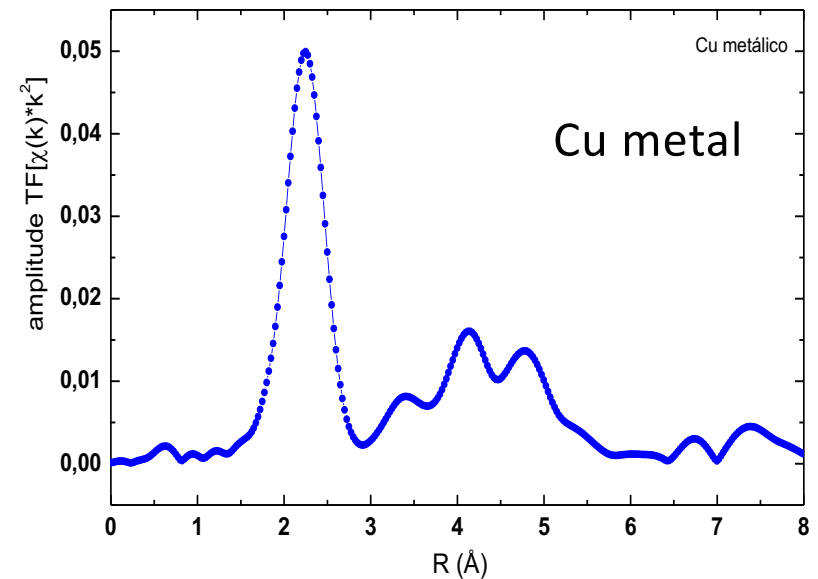
Farrel W. Lytle

Boeing Scientific Research Laboratories, Seattle, Washington 98124

(Received 16 July 1971)



Fourier
Transformation



Pseudo radial distribution function

EXAFS – Extended X-ray Absorption Fine Structure

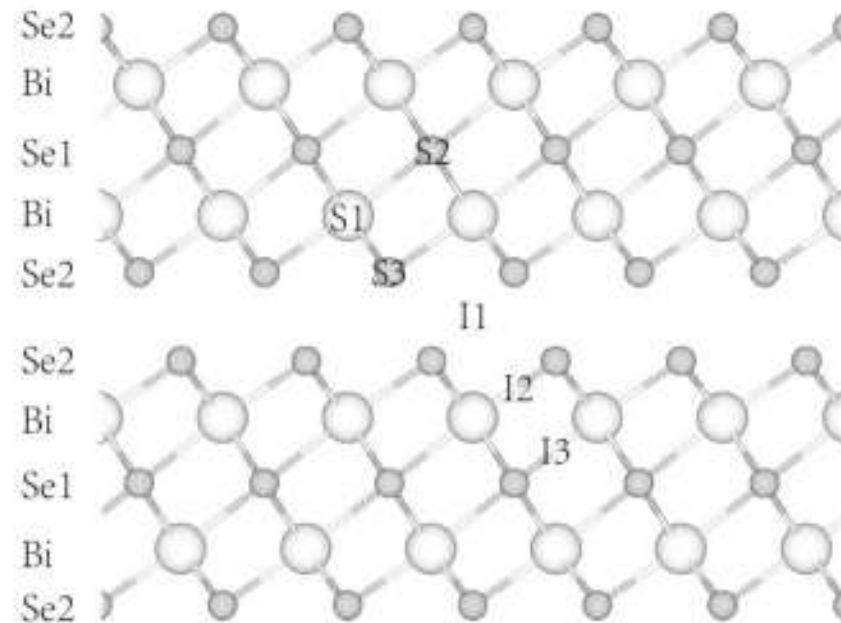
- Can be used to obtain structural parameters around the absorbing atom, as:
 - Number of neighbors
 - Interatomic distances
 - Debye-Waller factor
- It give the structural parameters locally around the absorbing atom
 - Does not require long range order
- It's often applied to:
 - Non-crystalline systems
 - Crystalline systems where some structural modifications are not long range ordered
 - Dopants

Example: EXAFS of Cr dopant on Bi_2Se_3

PHYSICAL REVIEW B **90**, 094107 (2014)

Local structures around $3d$ metal dopants in topological insulator Bi_2Se_3 studied by EXAFS measurements

Zhen Liu,¹ Xinyuan Wei,¹ Jiajia Wang,¹ Hong Pan,¹ Fuhao Ji,¹ Fuchun Xi,¹ Jing Zhang,² Tiandou Hu,² Shuo Zhang,³ Zheng Jiang,³ Wen Wen,³ Yuying Huang,³ Mao Ye,⁴ Zhongqin Yang,^{1,*} and Shan Qiao^{4,5,1}



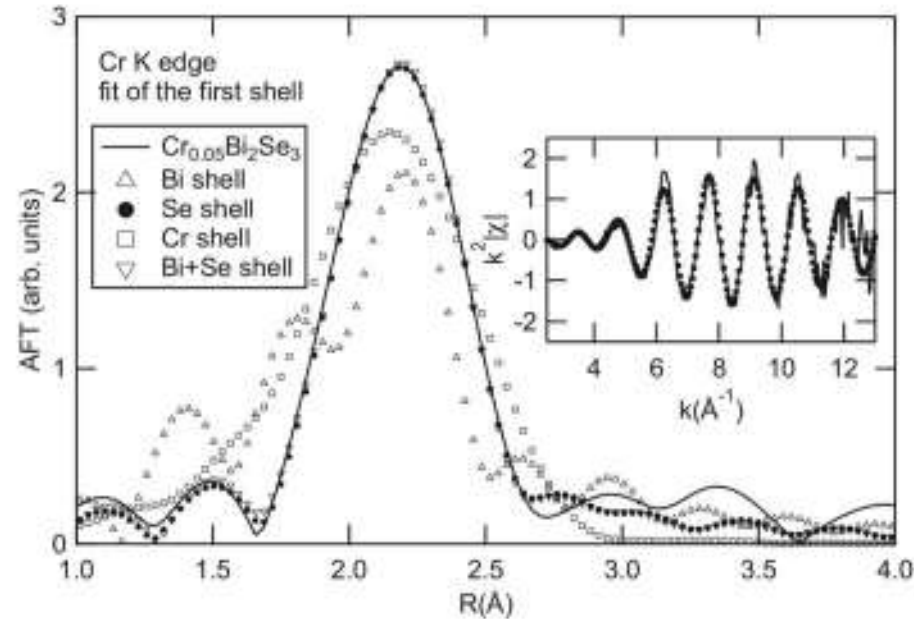
Example: EXAFS of Cr dopant on Bi_2Se_3 

TABLE III. The structural parameters from the first shell fittings with the models.

Model	Pair	R (Å)	N	S_0^2	ΔE (eV)	σ^2 (Å ²)	R factor
Bi shell	Cr-Bi	2.21 ± 0.01	3 ± 2	0.66	-4 ± 4	0.000 ± 0.003	7%
Cr shell	Cr-Cr	2.54 ± 0.04	8	0.66	-16 ± 7	0.006 ± 0.002	6%
	Cr-Cr	2.93 ± 0.04	6	0.66	-16 ± 7	0.006 ± 0.002	
Se shell	Cr-Se	2.50 ± 0.01	6	0.66	-1 ± 1	0.0033 ± 0.0002	0.2%
Bi+Se shell	Cr-Bi	2.50 ± 0.01	6 ± 1	0.66	-25 ± 10	0.06 ± 0.04	0.2%
	Cr-Se	2.50 ± 0.01	6 ± 1	0.66	-1 ± 1	0.0036 ± 0.0007	

Short-range charge order in $R\text{NiO}_3$ perovskites ($R=\text{Pr}, \text{Nd}, \text{Eu}, \text{Y}$) probed by x-ray-absorption spectroscopy

Cynthia Piamonteze,^{1,2} Hélio C. N. Tolentino,¹ Aline Y. Ramos,^{1,3} Nestor E. Massa,⁴ Jose A. Alonso,⁵ Maria J. Martínez-Lope,⁵ and Maria T. Casais⁵

¹Laboratório Nacional Luz Síncrotron, Caixa Postal 6192, 13084-971 Campinas/SP, Brazil

²IFGW/UNICAMP, 13083-970 Campinas/SP, Brazil

³LMCP-UMR, 7590 CNRS, Paris, France

⁴LANAIS, CEQUINOR, UNLP, C.C. 962, 1900 La Plata, Argentina

⁵Instituto de Ciencia de Materiales de Madrid, C.S.I.C., Cantoblanco, E-28049 Madrid, Spain

(Received 10 August 2004; published 25 January 2005)

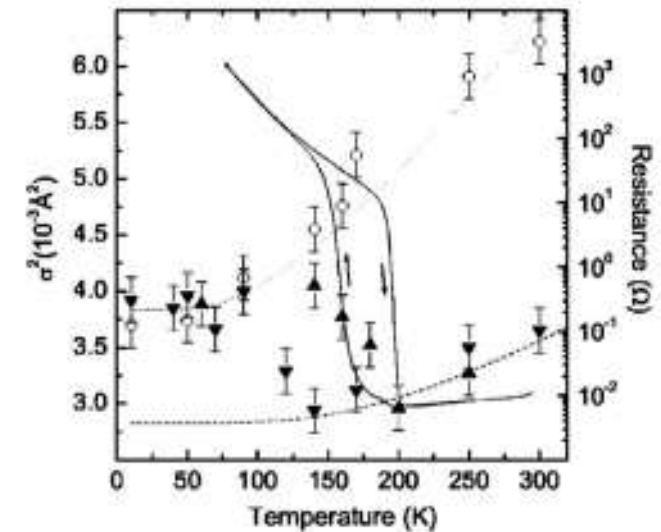
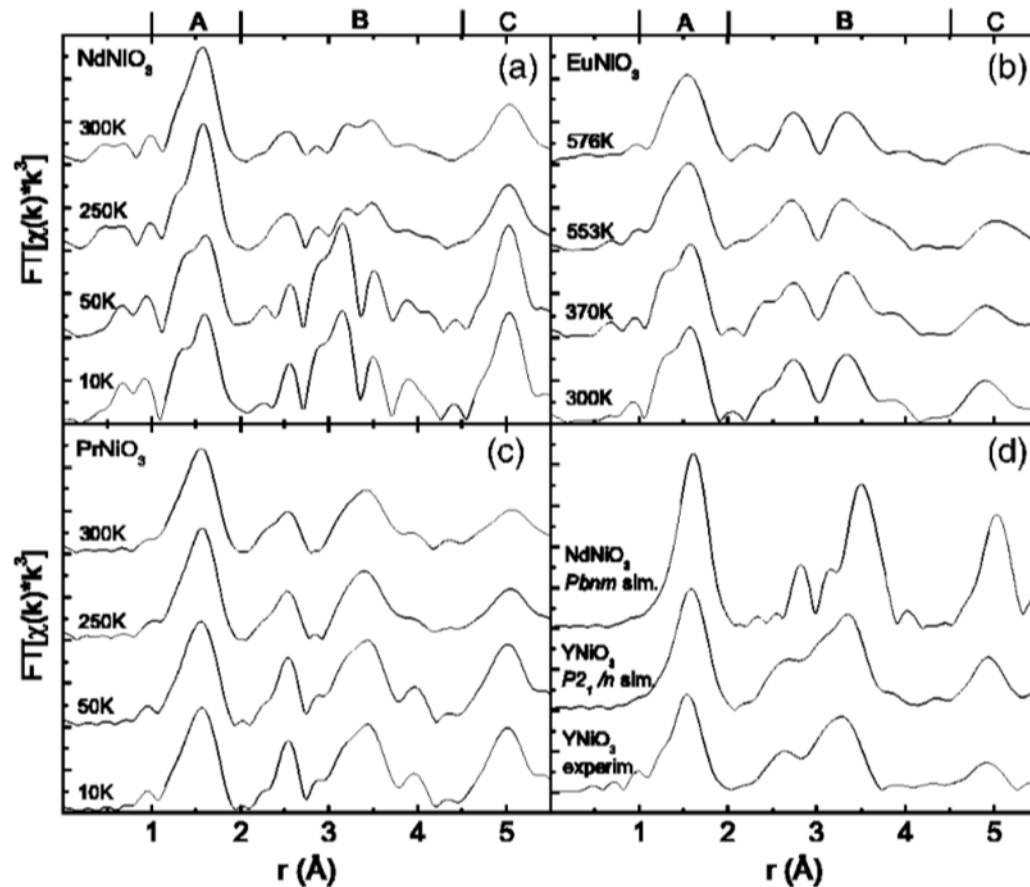


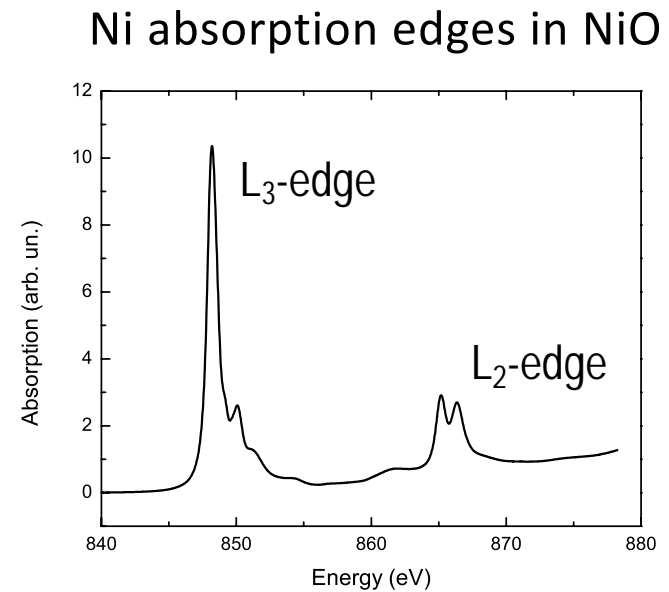
FIG. 3. Total disorder for the NdNiO_3 coordination shell while decreasing (\blacktriangledown) and increasing (\blacktriangle) the temperature, and for Ni shell at 5 Å (\circ). Thermal behavior for the coordination shell ($---$) and Ni shell ($- \cdot - \cdot -$), and resistance ($-$).



Transition Metal L-edges

Why should one study the transition metal L-edges?

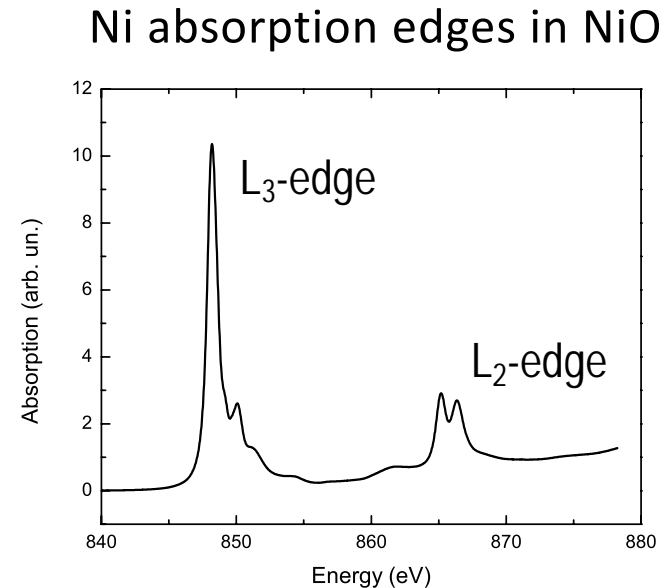
L_{2,3} edges:
2p core state
transition 2p → 3d



Why should one study the transition metal L-edges?

Why should one study the transition metal L-edges?

L_{2,3} edges:
2p core state
transition 2p → 3d



Why should one study the transition metal L-edges?

- 3d band
- the valence band => valence state
- outer most band => ligand field
- Partially filled => magnetism



Soft X-ray range (400eV-2000eV)

- K-edges: 1s → 4p
- L_{2,3}-edges: 2p → 3d
- M_{2,3}-edges: 3p → 4d
- M_{4,5}-edges: 3d → 4f

1	2	3	4	5	6	7	8	9	10	11	12	13	14	15	16	17	18	
hydrogen 1 H 1.0079																	helium 2 He 4.0026	
lithium 3 Li 6.941	beryllium 4 Be 9.0122											boron 5 B 10.811	carbon 6 C 12.011	nitrogen 7 N 14.007	oxygen 8 O 15.999	fluorine 9 F 18.998	neon 10 Ne 20.180	
sodium 11 Na 22.990	magnesium 12 Mg 24.305											aluminum 13 Al 26.982	silicon 14 Si 28.086	phosphorus 15 P 30.974	sulfur 16 S 32.065	chlorine 17 Cl 35.453	argon 18 Ar 39.948	
potassium 19 K 39.098	calcium 20 Ca 40.078	scandium 21 Sc 44.956	titanium 22 Ti 47.867	vanadium 23 V 50.942	chromium 24 Cr 51.996	manganese 25 Mn 54.938	iron 26 Fe 55.845	cobalt 27 Co 58.933	nickel 28 Ni 58.693	copper 29 Cu 63.546	zinc 30 Zn 65.38	gallium 31 Ga 69.723	germanium 32 Ge 72.61	arsenic 33 As 74.922	selenium 34 Se 78.96	bromine 35 Br 79.904	krypton 36 Kr 83.80	
rubidium 37 Rb 85.468	strontium 38 Sr 87.62	yttrium 39 Y 88.906	zirconium 40 Zr 91.224	niobium 41 Nb 92.906	molybdenum 42 Mo 95.94	technetium 43 Tc [98]	ruthenium 44 Ru 101.07	rhodium 45 Rh 102.91	palladium 46 Pd 106.42	silver 47 Ag 107.87	cadmium 48 Cd 112.41	indium 49 In 114.82	tin 50 Sn 118.71	antimony 51 Sb 121.76	tellurium 52 Te 127.60	iodine 53 I 126.90	xenon 54 Xe 131.29	
cesium 55 Cs 132.91	barium 56 Ba 137.33	*lanthanoids 57-70 ***	lutetium 71 Lu 174.97	hafnium 72 Hf 178.49	tantalum 73 Ta 180.95	tungsten 74 W 183.84	rhenium 75 Re 186.21	osmium 76 Os 190.23	iridium 77 Ir 192.22	platinum 78 Pt 195.08	gold 79 Au 196.97	mercury 80 Hg 200.59	thallium 81 Tl 204.38	lead 82 Pb 207.2	bismuth 83 Bi 208.98	polonium 84 Po [209]	astatine 85 At [210]	radon 86 Rn [222]
francium 87 Fr [223]	radium 88 Ra [226]	**actinoids 89-102 ***	lawrencium 103 Lr [262]	rutherfordium 104 Rf [267]	dubnium 105 Db [268]	seaborgium 106 Sg [271]	bohrium 107 Bh [272]	hassium 108 Hs [270]	meitnerium 109 Mt [276]	darmstadtium 110 Ds [281]	roentgenium 111 Rg [289]	unbinium 112 Uub [285]	ununium 113 Uut [284]	ununium 114 Uuq [289]	ununium 115 Uup [288]	ununium 116 Uuh [293]	ununium 117 Uus [294]	ununium 118 Uuo [294]

3d, 4d ←

4p

4f ←

*lanthanoids

**actinoids

lanthanum 57 La 138.91	cerium 58 Ce 140.12	praseodymium 59 Pr 140.91	neodymium 60 Nd 144.24	promethium 61 Pm [145]	samarium 62 Sm 150.36	europium 63 Eu 151.96	gadolinium 64 Gd 157.25	terbium 65 Tb 158.93	dysprosium 66 Dy 162.50	holmium 67 Ho 164.93	erbium 68 Er 167.26	thulium 69 Tm 168.93	ytterbium 70 Yb 173.05
actinium 89 Ac [227]	thorium 90 Th 232.04	protactinium 91 Pa 231.04	uranium 92 U 238.03	neptunium 93 Np [237]	plutonium 94 Pu [244]	americium 95 Am [243]	curium 96 Cm [247]	berkelium 97 Bk [247]	californium 98 Cf [251]	einsteinium 99 Es [252]	fermium 100 Fm [257]	mendelevium 101 Md [258]	nobelium 102 No [259]

K-edge quadrupolar transition

Fe K-edge in different compounds

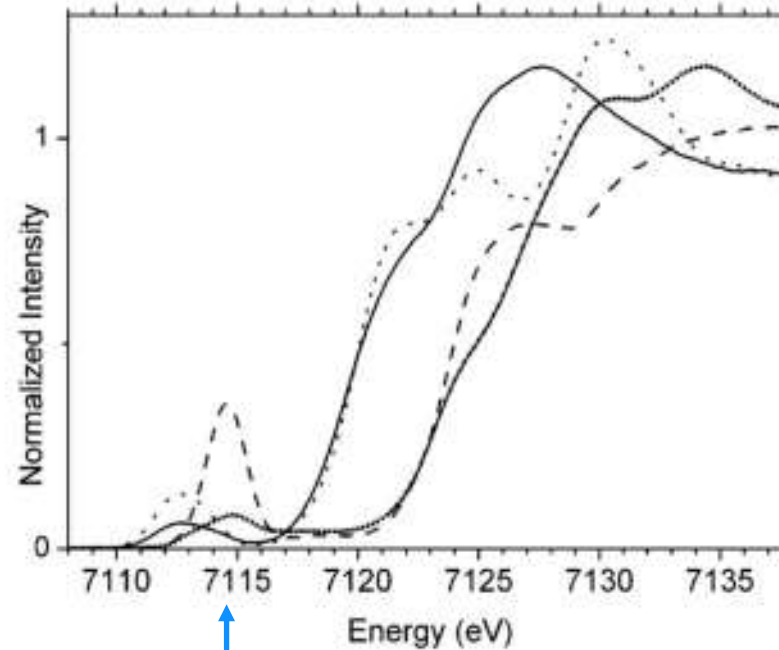
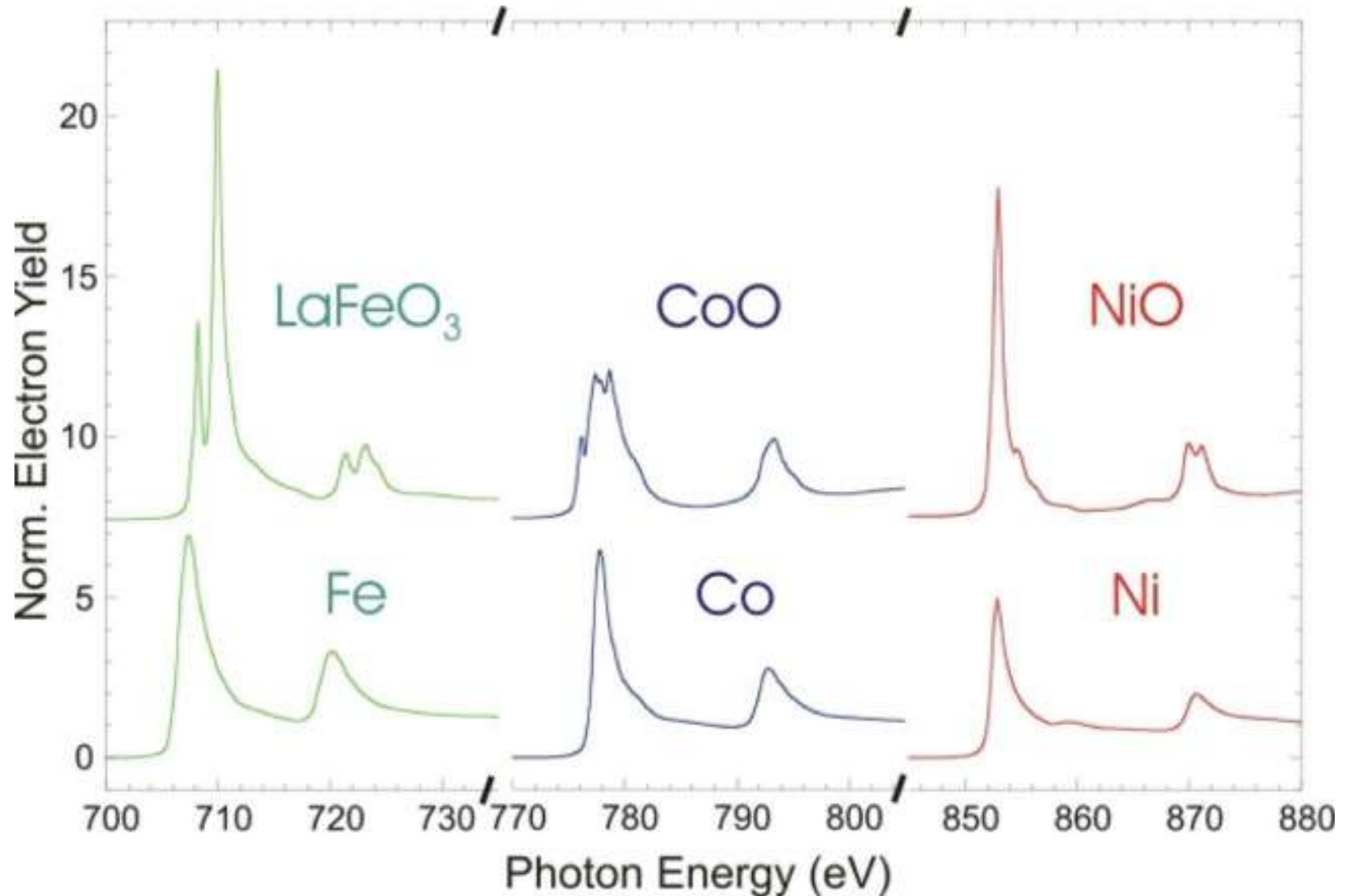


Figure 5. Experimental Fe 1s X-ray absorption spectra of (a) FeAl₂O₄ (dotted), (b) Fe₂SiO₄ (solid), (c) Fe₂O₃ (solid with points), and (d) FePO₄ (dashed).

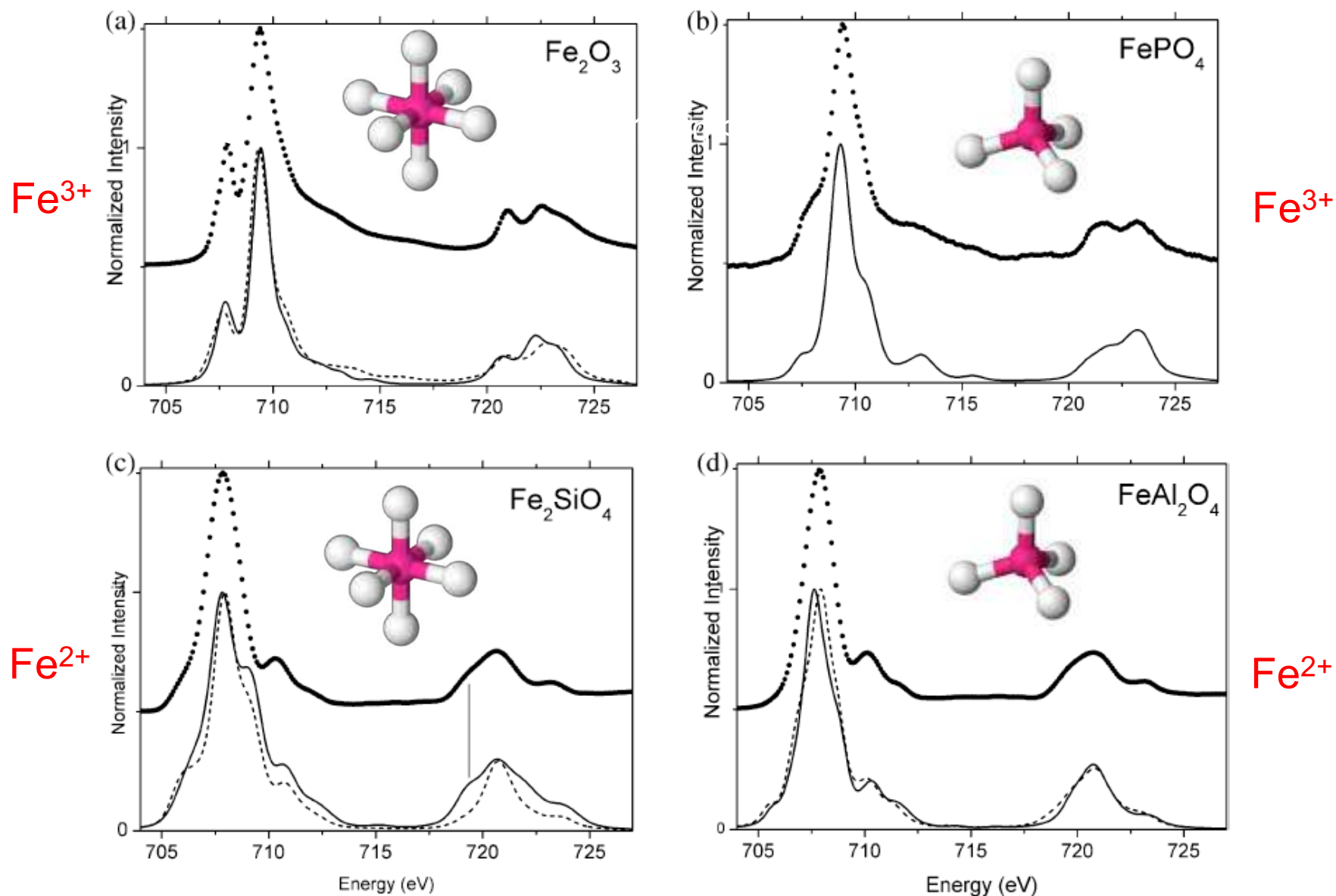
Quadrupolar transition 1s -> 3d

XAS Spectra: oxides x metals

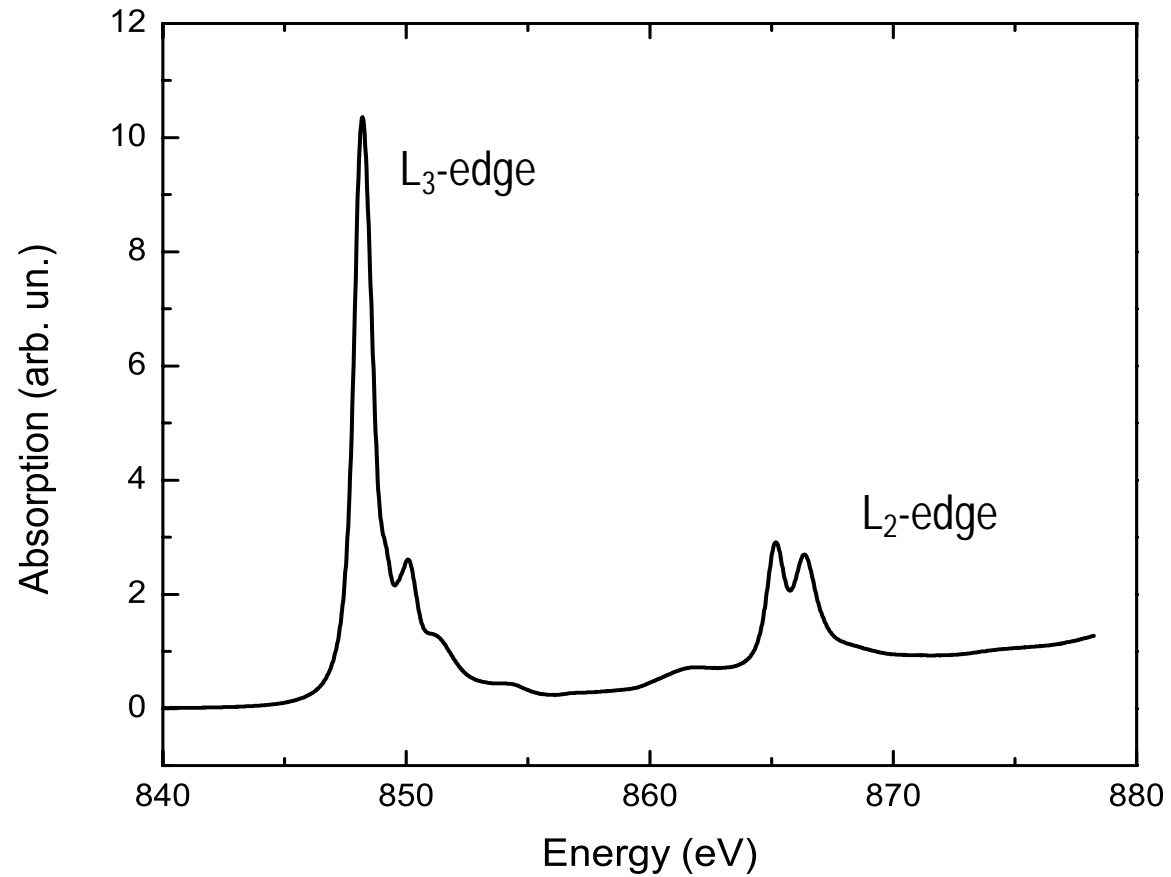
Where does the fine structure from oxides come from?



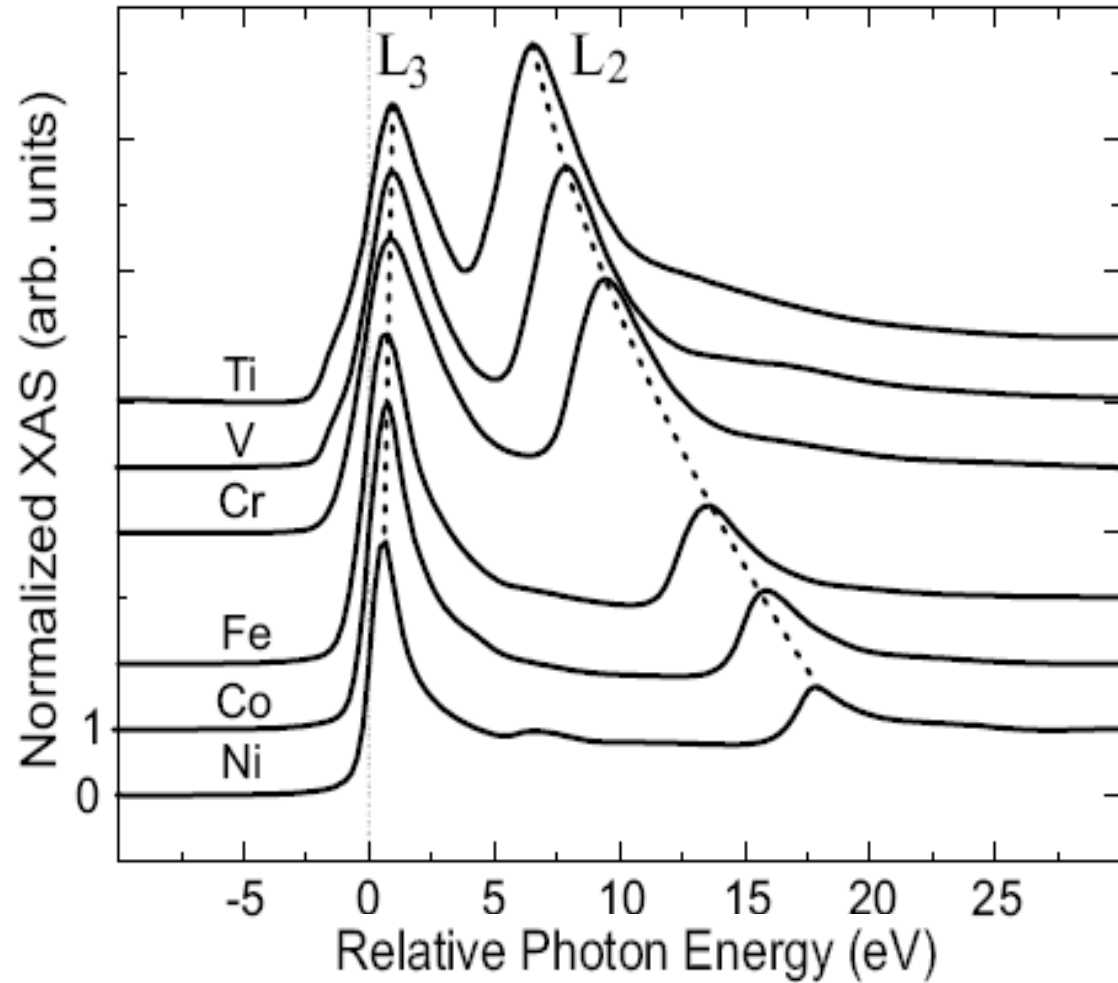
Information contained in the XA Spectra



Why are there two edges?



Element	ζ_{2p} (eV)
Mn	6.8
Fe	8.2
Co	9.8
Ni	11.5
Cu	13.5

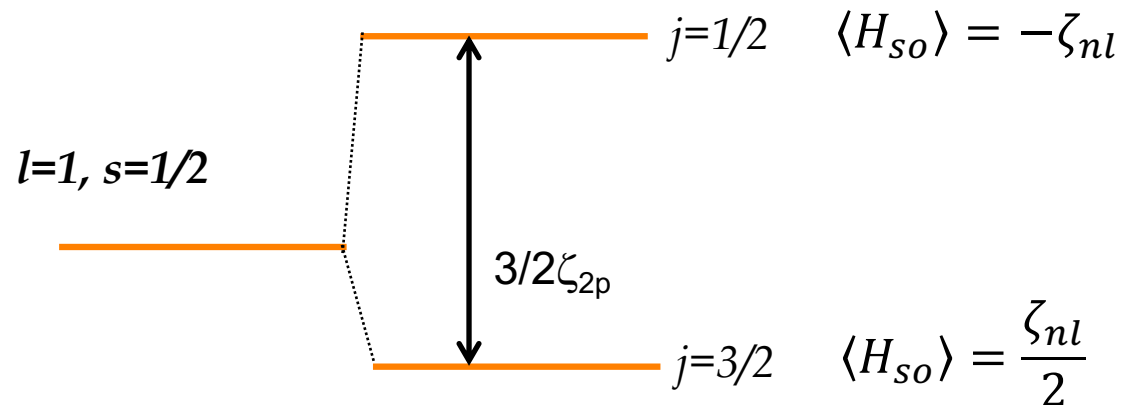


For comparison, 3d spin-orbit $\sim 100\text{meV}$

L₃ and L₂ edges: Spin-Orbit Coupling

- L_{2,3} edges:
 - transition 2p → 3d
- Spin-orbit coupling for a 2p hole:
 - l=1
 - s=1/2
 - j=l+s ... l-s = **3/2, 1/2**

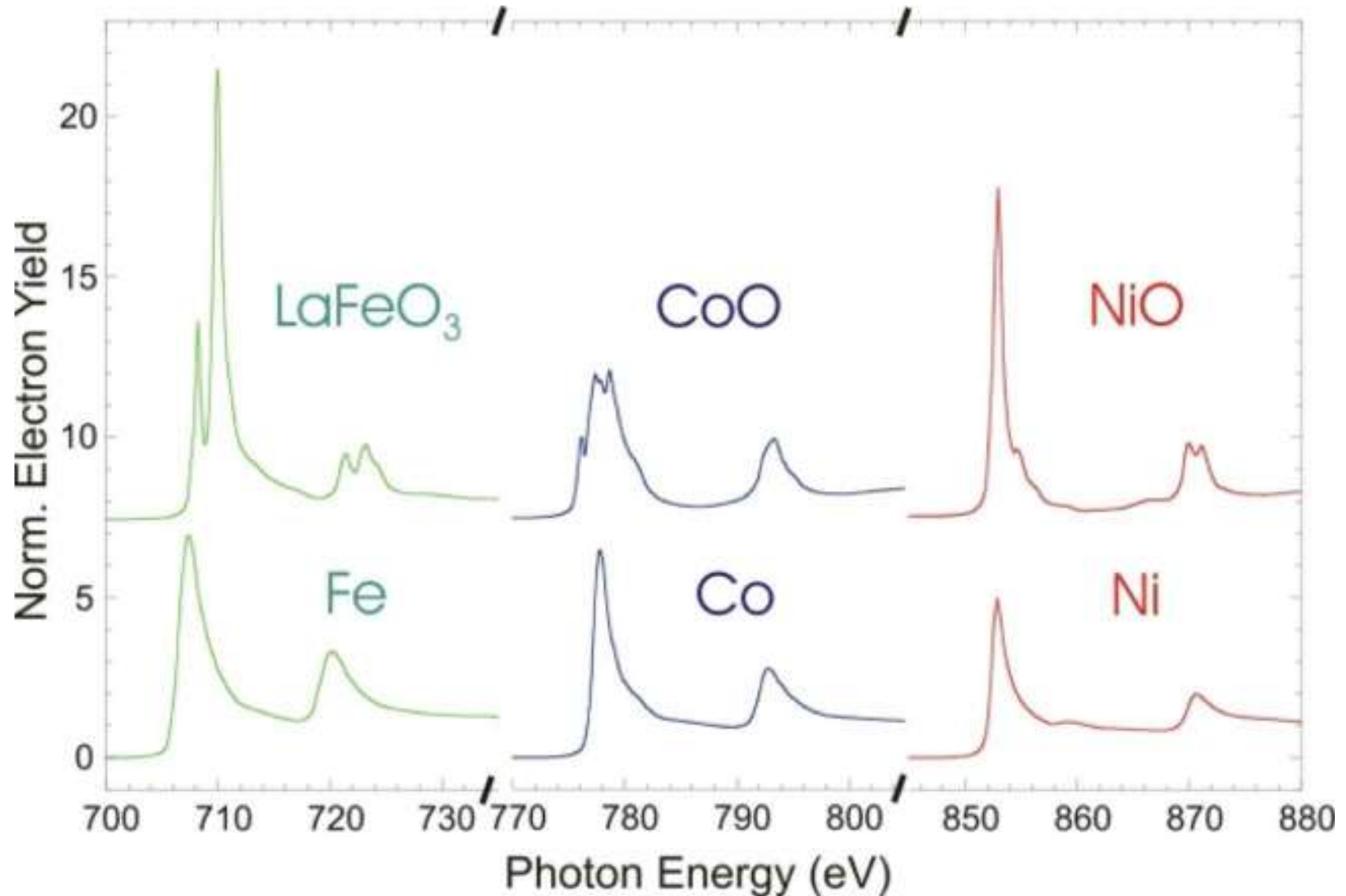
$$\langle H_{so} \rangle = \frac{\zeta_{nl}}{2} [j(j+1) - l(l+1) - s(s+1)]$$



$\zeta_{nl} < 0$, for more than half filled shell

XAS Spectra: oxides x metals

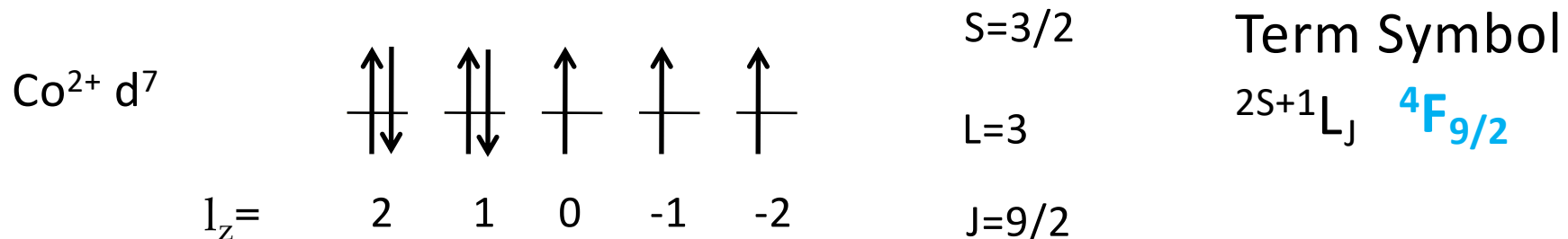
Where does the fine structure from oxides come from?



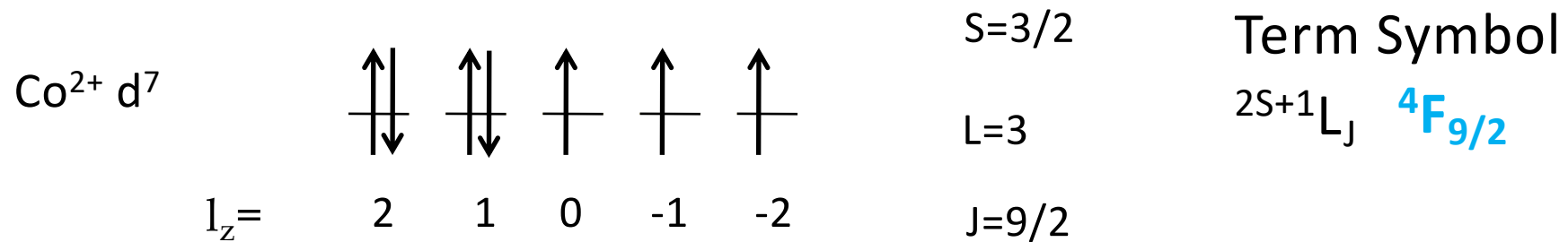
Ground state of partially filled shells

Hund's rule

- How to define the ground state of a partially filled shell?
- For example: Co^{2+} has 7 electrons in the d-shell.
- Hund's rules:
 - 1st: Lowest electronic state has largest total spin **S**
Pauli's exclusion principle => minimizes Coulomb interaction
 - 2nd: Lowest electronic state has largest total orbital moment **L**
Electrons circulating in the same direction (parallel angular momentum)
=> minimizes Coulomb interaction
 - 3rd: Lowest electronic state has largest total angular momentum **J**, if shell is more than half full or smallest total angular momentum **J**, if the shell is less than half full



XAS: how does the final state looks like?



Final state XAS at Co L_{2,3}-edges in Co²⁺

2p⁵3d⁸

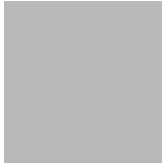
Example: XAS of Ti^{4+}

- Initial state $2p^63d^0$
 - 1S_0
- Final state: $2p^53d^1$, same as $2p3d$
 - $S_1=1/2, S_2=1/2, S_{\text{total}}=0,1$
 - $L_1=1, L_2=2, L_{\text{total}}=1,2,3$
 - $J=L-S \dots L+S$

Term Symbol:
$2S+1 L_{2J+1}$

L/S	0	1
1	1P_1	$^3P_0, ^3P_1, ^3P_2$
2	1D_2	$^3D_1, ^3D_2, ^3D_3$
3	1F_3	$^3F_2, ^3F_3, ^3F_4$

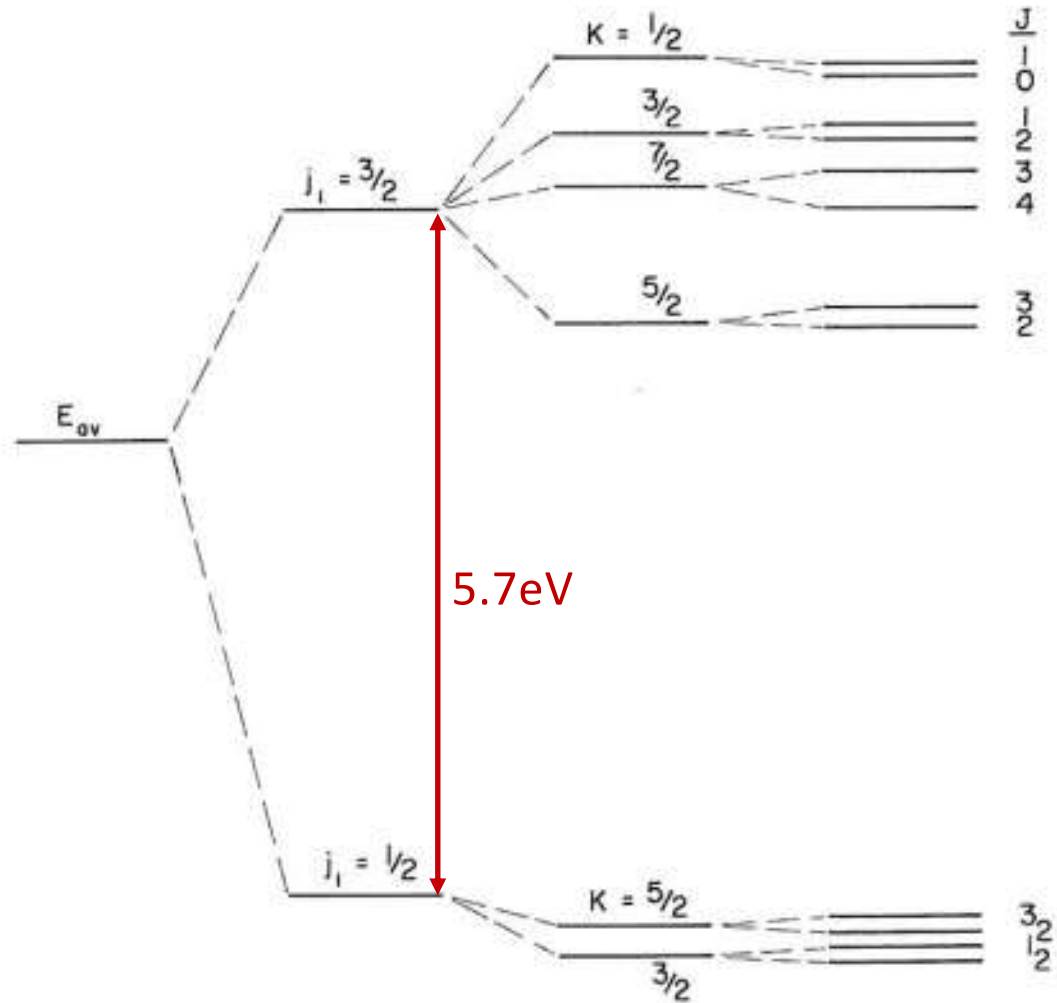
There are 12 different configurations for pd!



Ti⁴⁺: d⁰

XAS final state:

2p⁵3d¹



Sph.
ave.

+

2p spin-orbit

Coulomb
direct

+

Coulomb
Exchange

+

3d spin-orbit

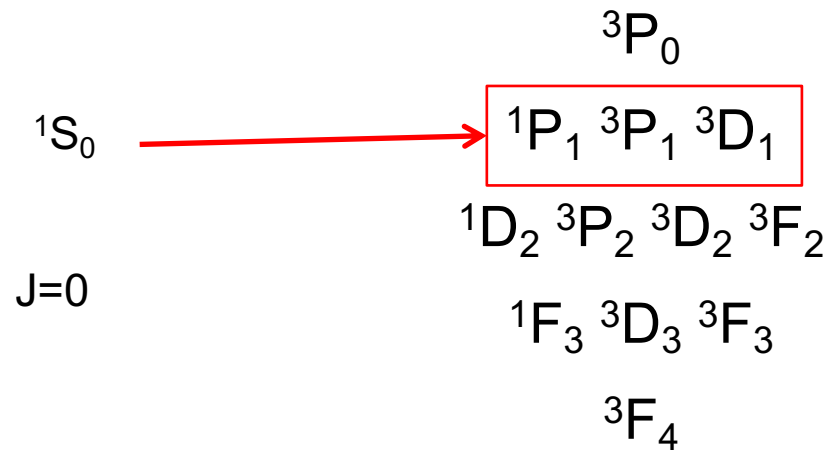
Dipole Selection rules

- Dipole Selection Rules:
 - $\Delta J = \pm 1, 0$ (except for $J=0$)

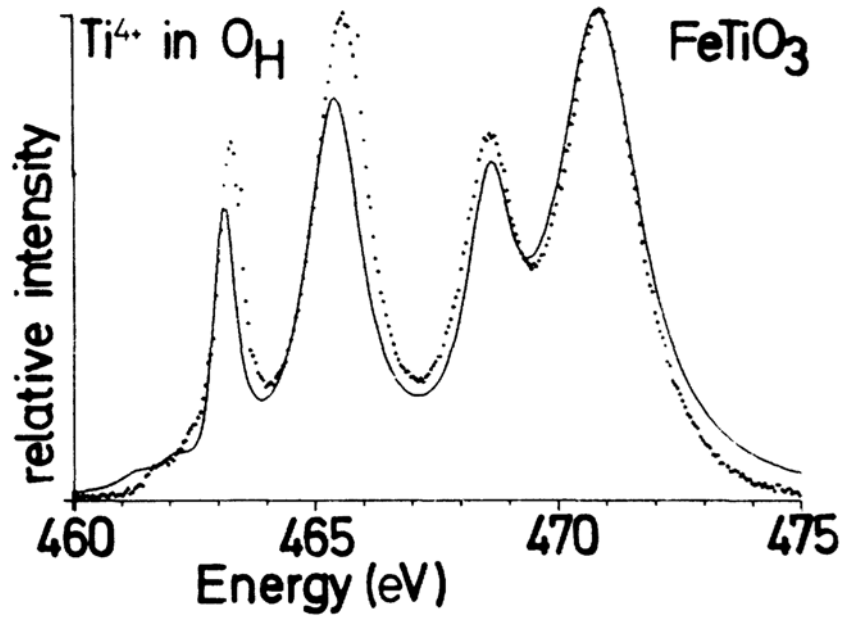
Ti⁴⁺ (2p⁶3d⁰) GS:

Ti⁴⁺ (2p⁵3d¹)

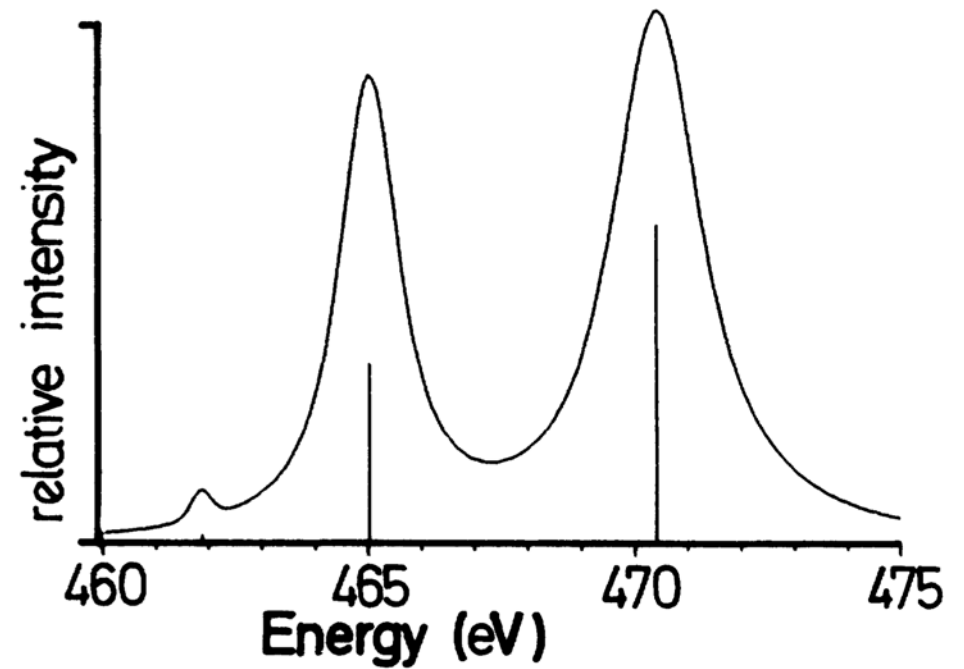
XAS final states:



What is missing?



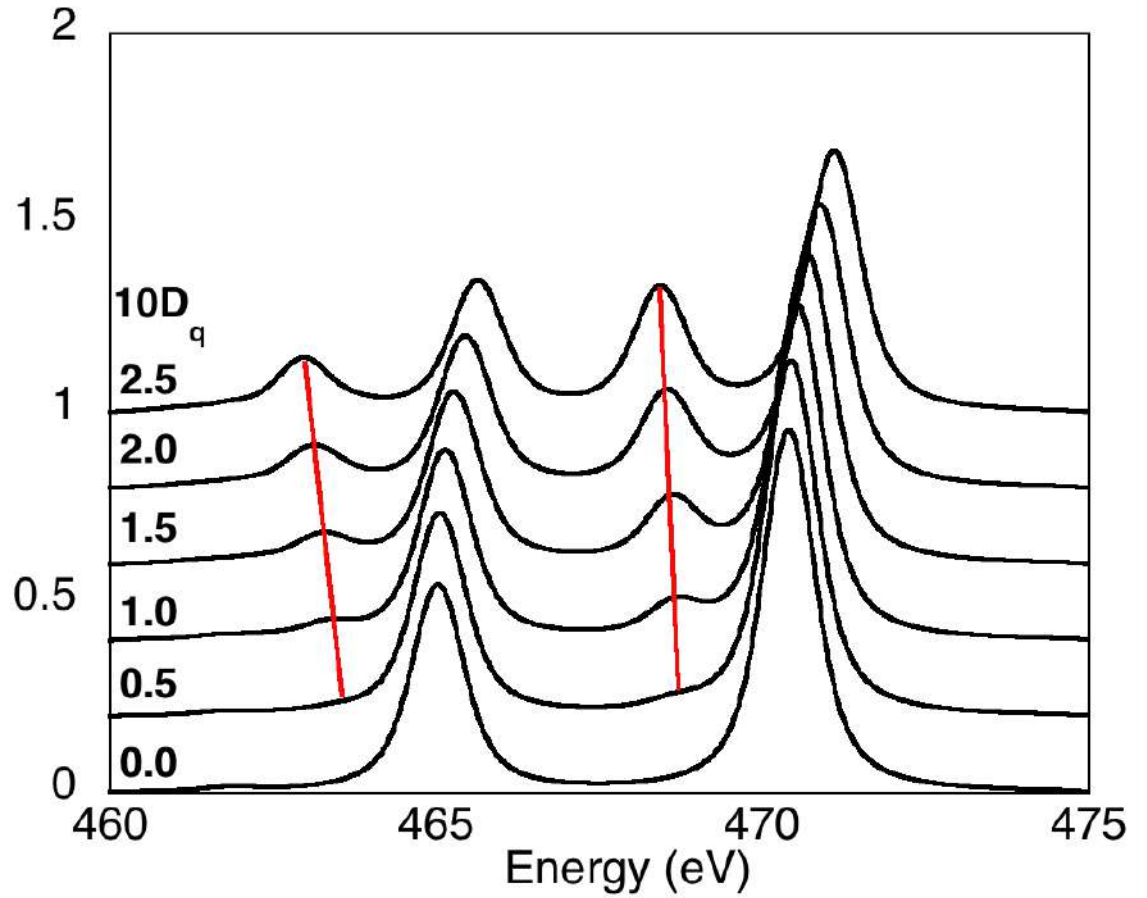
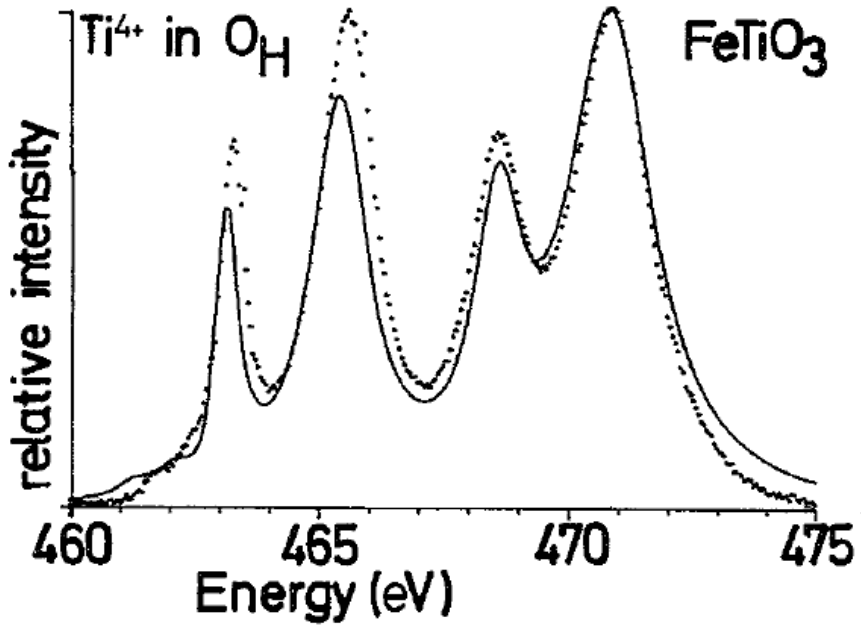
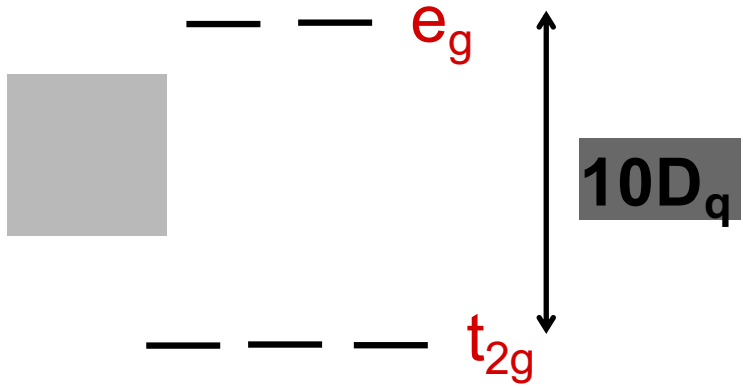
Measured Ti⁴⁺ XAS



F. M. F. de Groot *et al.* PRB **41**, 928 (1990).


Simulation of Ti⁴⁺ XAS

Ti⁴⁺: Inclusion of Crystal Field Splitting



(Some) x-ray absorption simulation codes suitable when multiplet structure is important

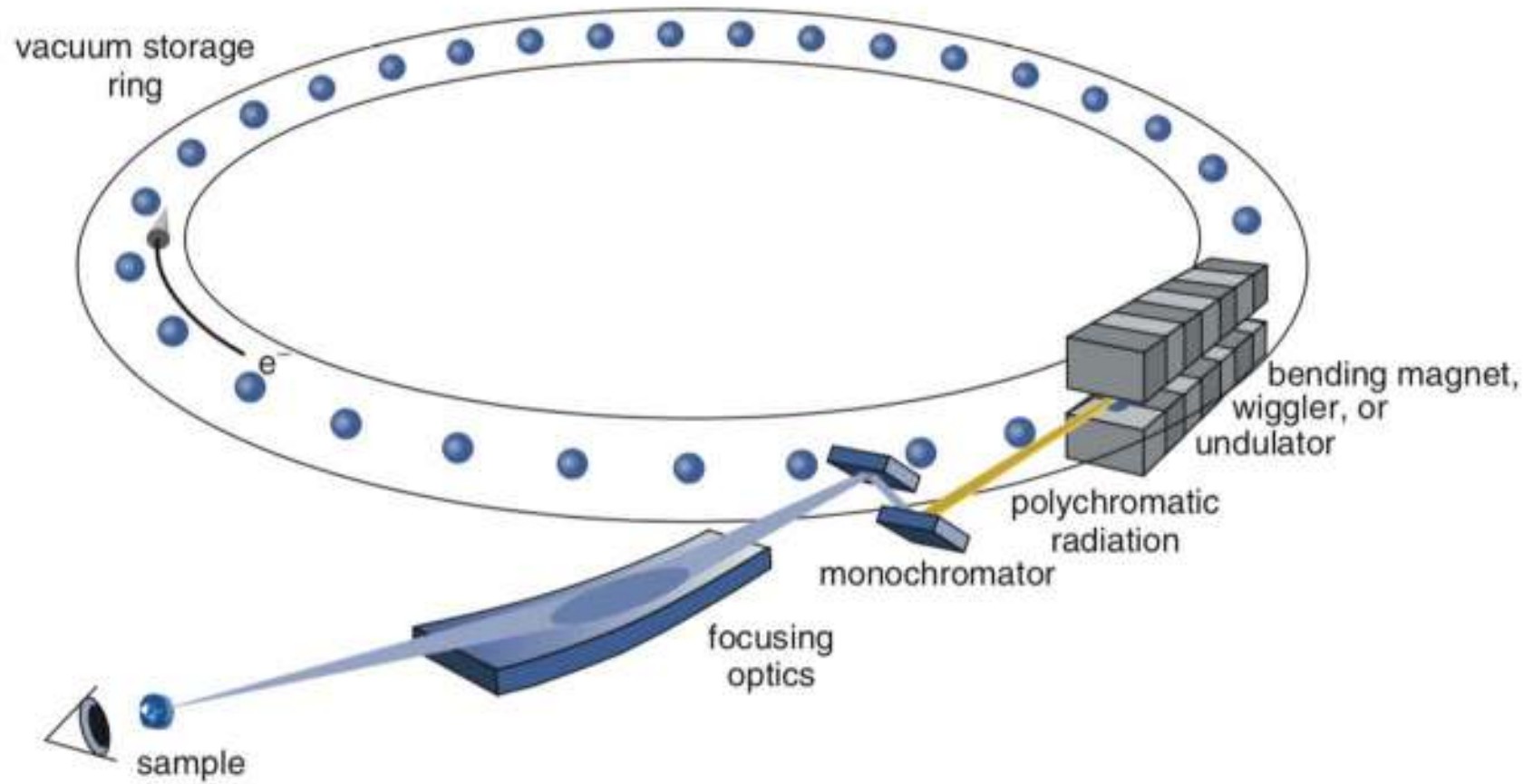
- CTM4XAS (<http://www.anorg.chem.uu.nl/CTM4XAS/>)
 - User friendly. Input: crystal field parameters and charge transfer parameters when necessary
- Quanty (<http://www.quanty.org/>)
 - More advanced. Possible to include DFT calculations output as input for the multiplet code
- MultiX (<http://multiplets.web.psi.ch/>)
 - Input parameter is the crystal structure. No inclusion of charge transfer
- **Multiplet structure is typically important for:**
 - **$L_{2,3}$ -edges of transition metal oxides. Metallic system often show no multiplet structure**
 - **$M_{4,5}$ edges of lanthanides**

- 
- A solid grey square is positioned to the left of the first bullet point.
- K edge probes p states
 - $L_{2,3}$ edges probe d states
 - The $L_{2,3}$ edges are split in two due to 2p spin-orbit coupling
 - Since the 3d states are partially localized electronic correlations are important to describe the spectrum
 - The L-edge spectrum is sensitive to the ligand field around the absorbing atom

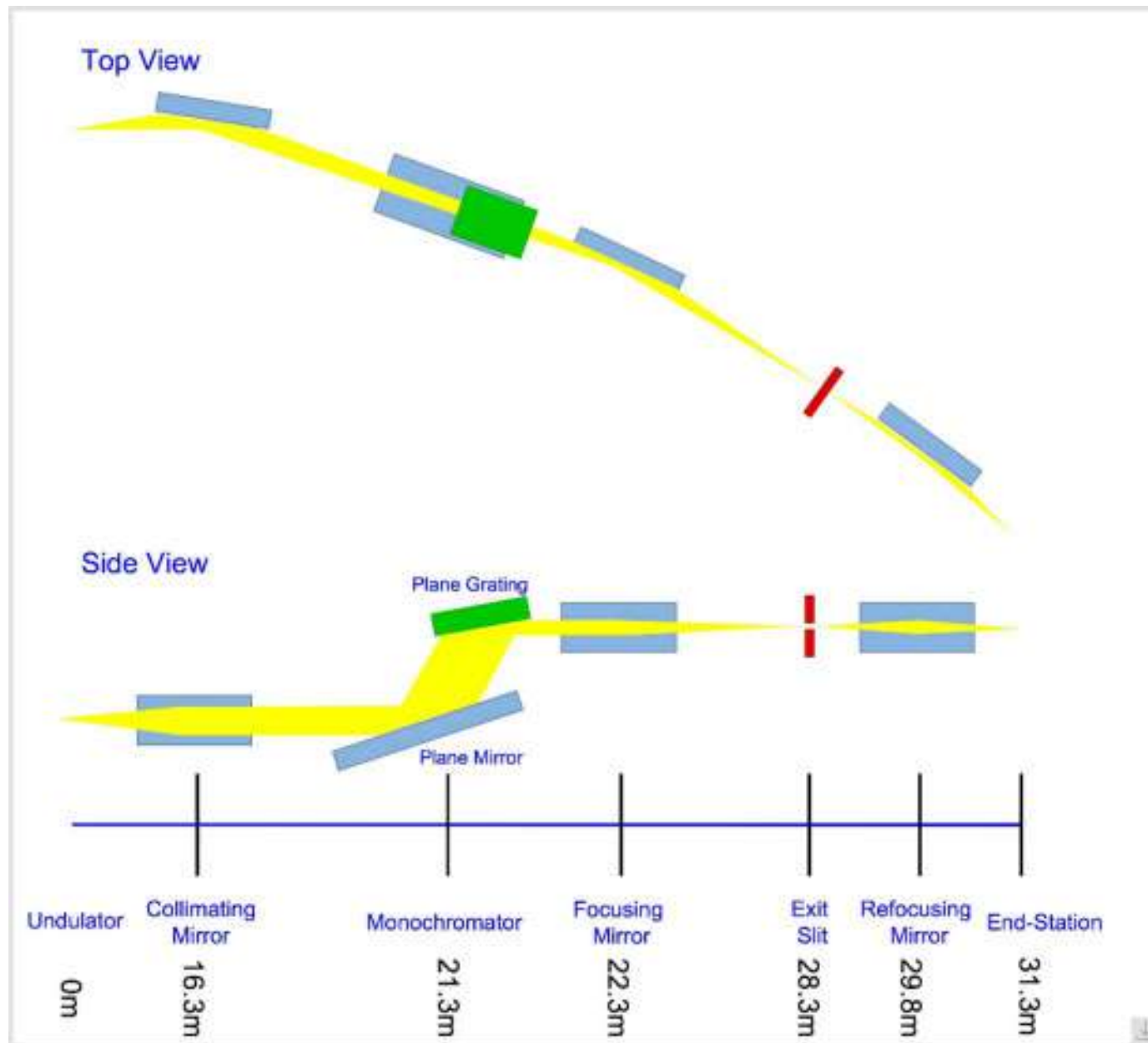


How to measure

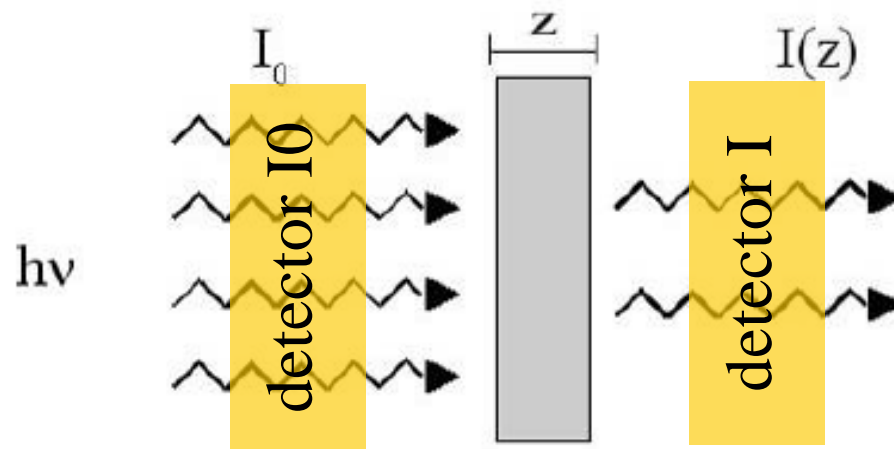
Synchrotron + beamline



Beamline Optics



X-ray absorption detection



transmission is the most direct

... but not always possible:

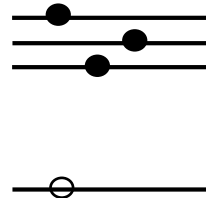
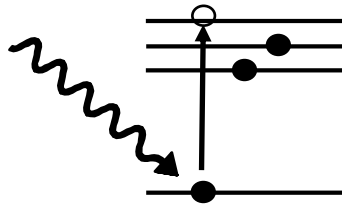
- Limitation on sample thickness
- Low contrast in very dilute systems

Decay channels

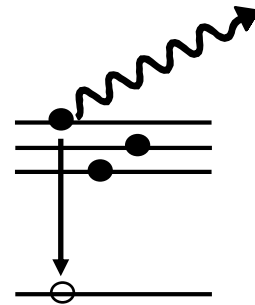


Initial

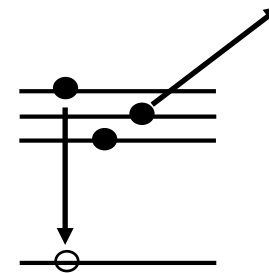
excited



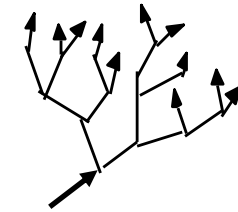
fluorescence



Auger



Secondary electrons



Soft X-ray range: ~ 5% fluorescence

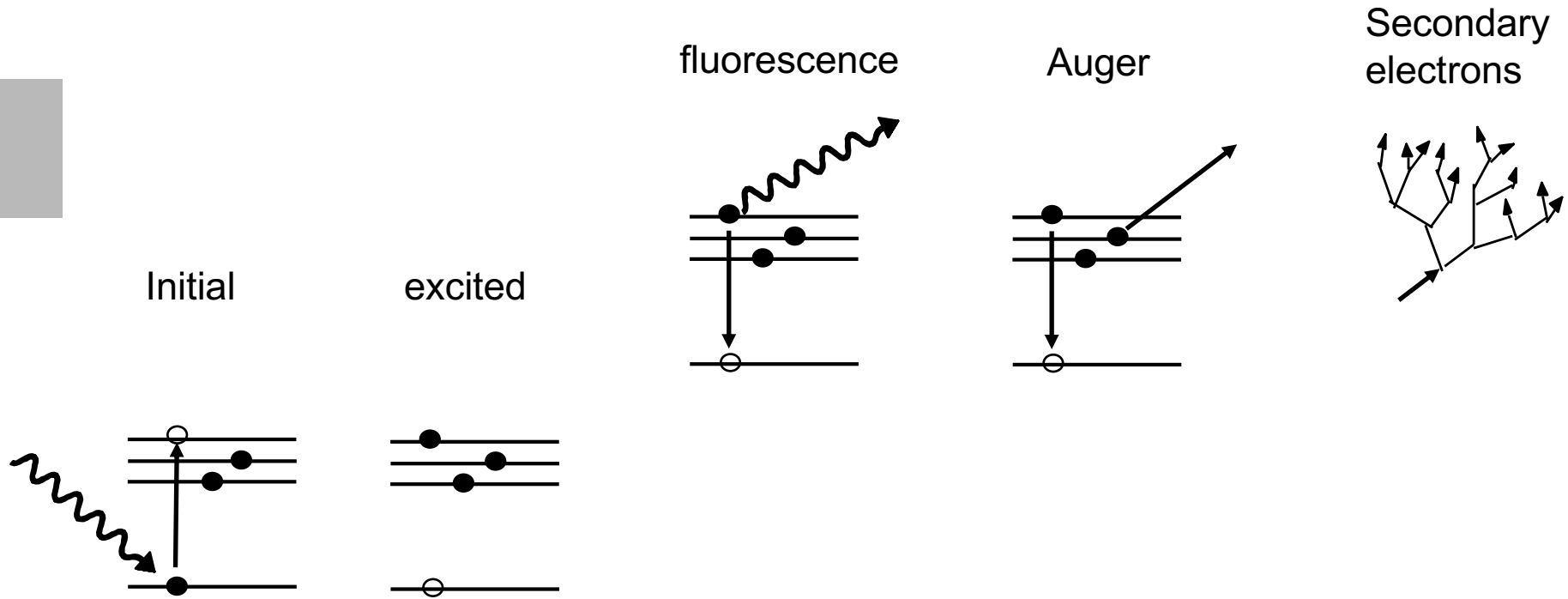
~ 95% Auger

Probing depth in soft X-rays:

Fluorescence:

TEY:

Decay channels

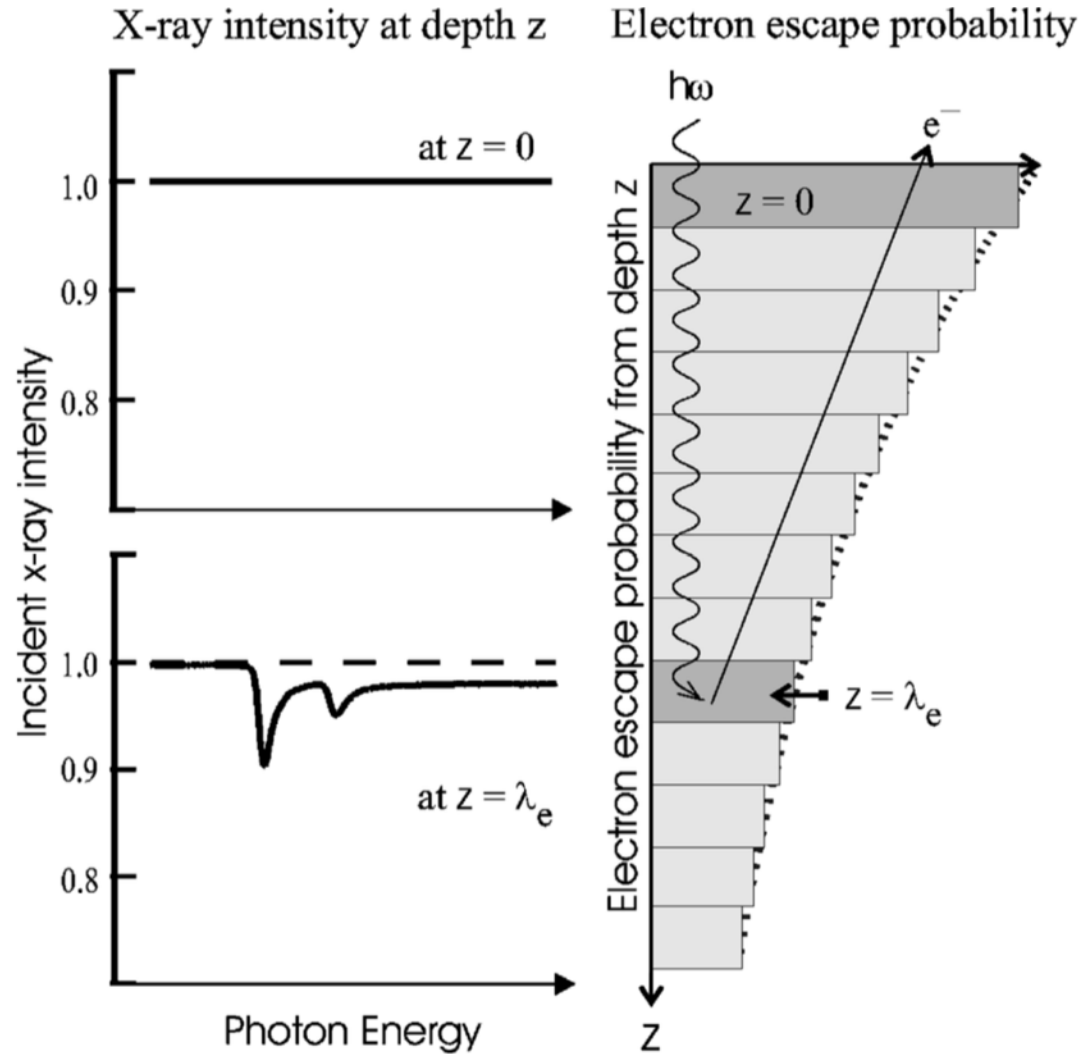


Probing depth in soft X-rays:

Fluorescence: $\lambda_x \sim 100\text{nm}$

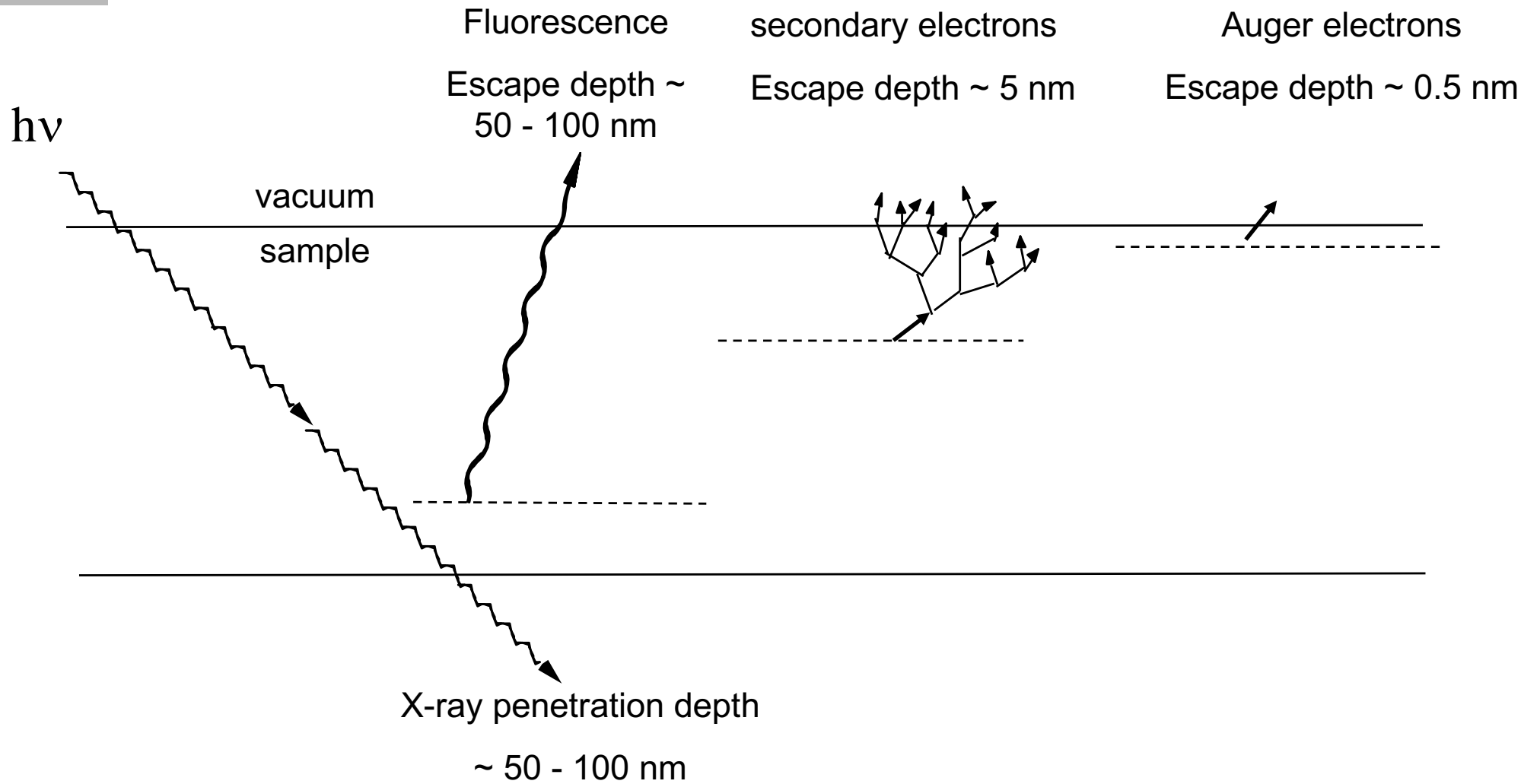
TEY: $\lambda_e \sim 2-5\text{nm}$

Meaning of p robing depth



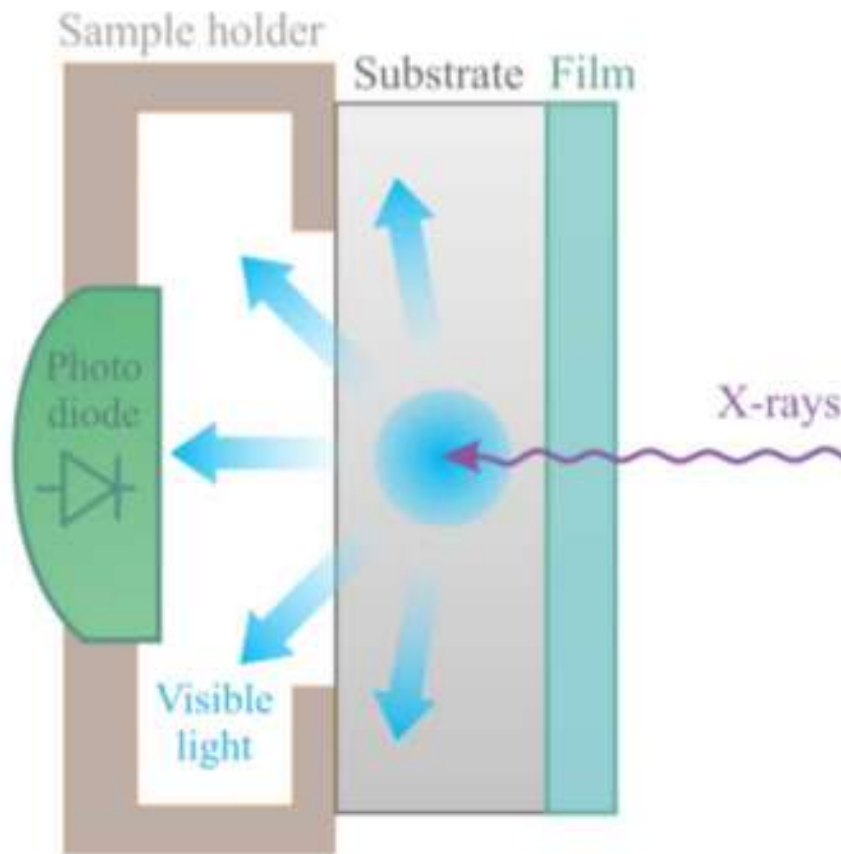
Detection methods

Sampling depth



X-ray excited optical luminescence

Y. W. Windsor et al, PRB **95**, 357 (2017).

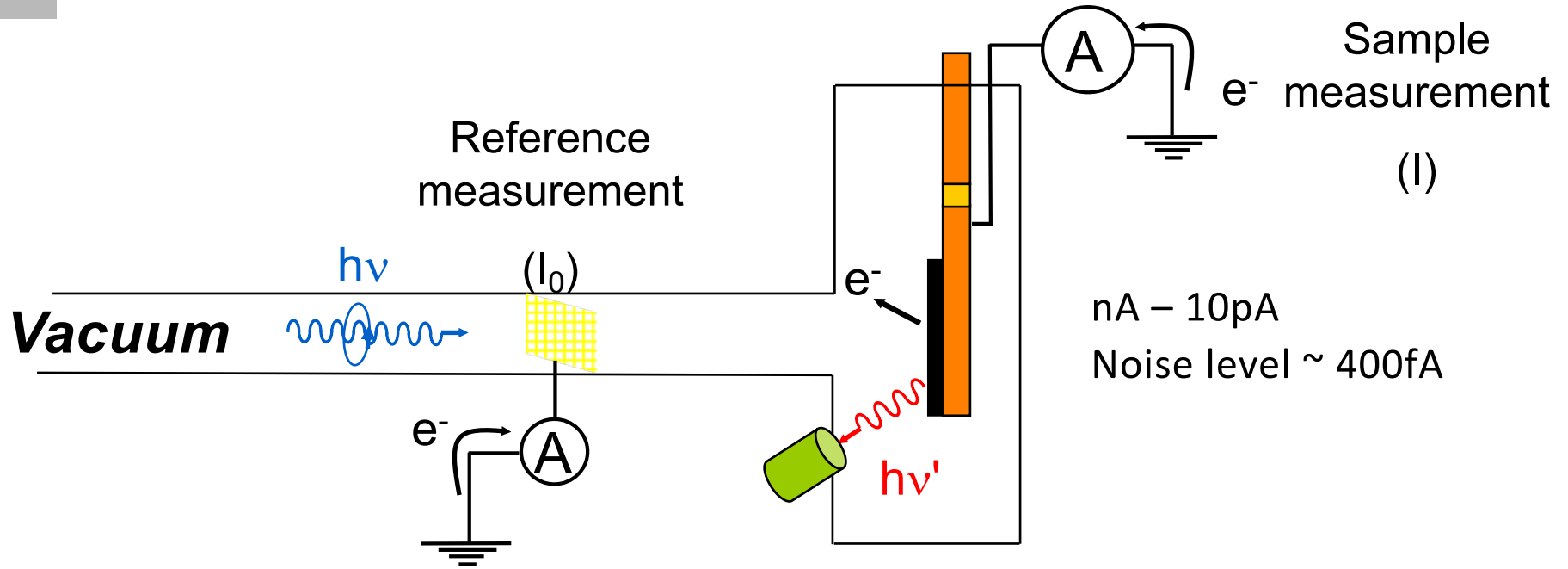


Allows transmission like measurements of X-rays in thin films

X-ray penetration depth

~ 100 nm

Scheme of a Experimental Setup





Examples

COMMUNICATION

Magnetic Thin Films

ADVANCED
MATERIALS

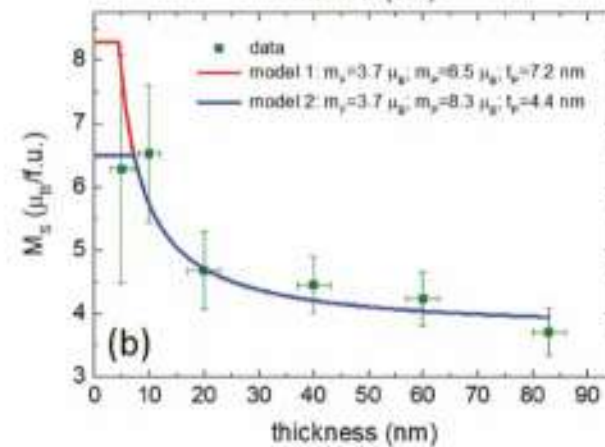
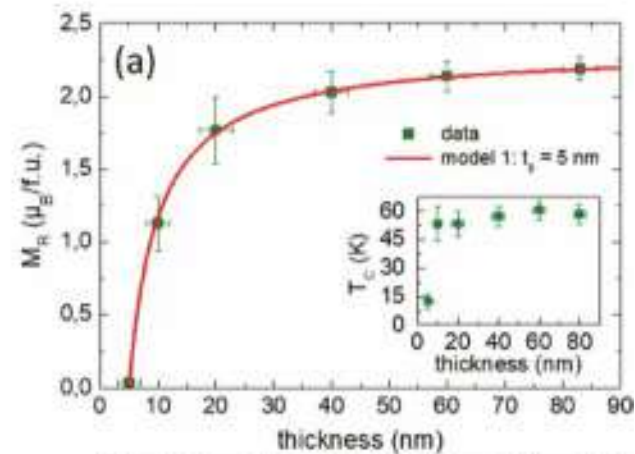
www.advmat.de

A Living-Dead Magnetic Layer at the Surface of Ferrimagnetic DyTiO₃ Thin Films

Raphaël Aeschlimann, Daniele Preziosi, Philipp Scheiderer, Michael Sing, Sergio Valencia, Jacobo Santamaria, Chen Luo, Hanjo Ryll, Florin Radu, Ralph Claessen, Cinthia Piamonteze, and Manuel Bibes*

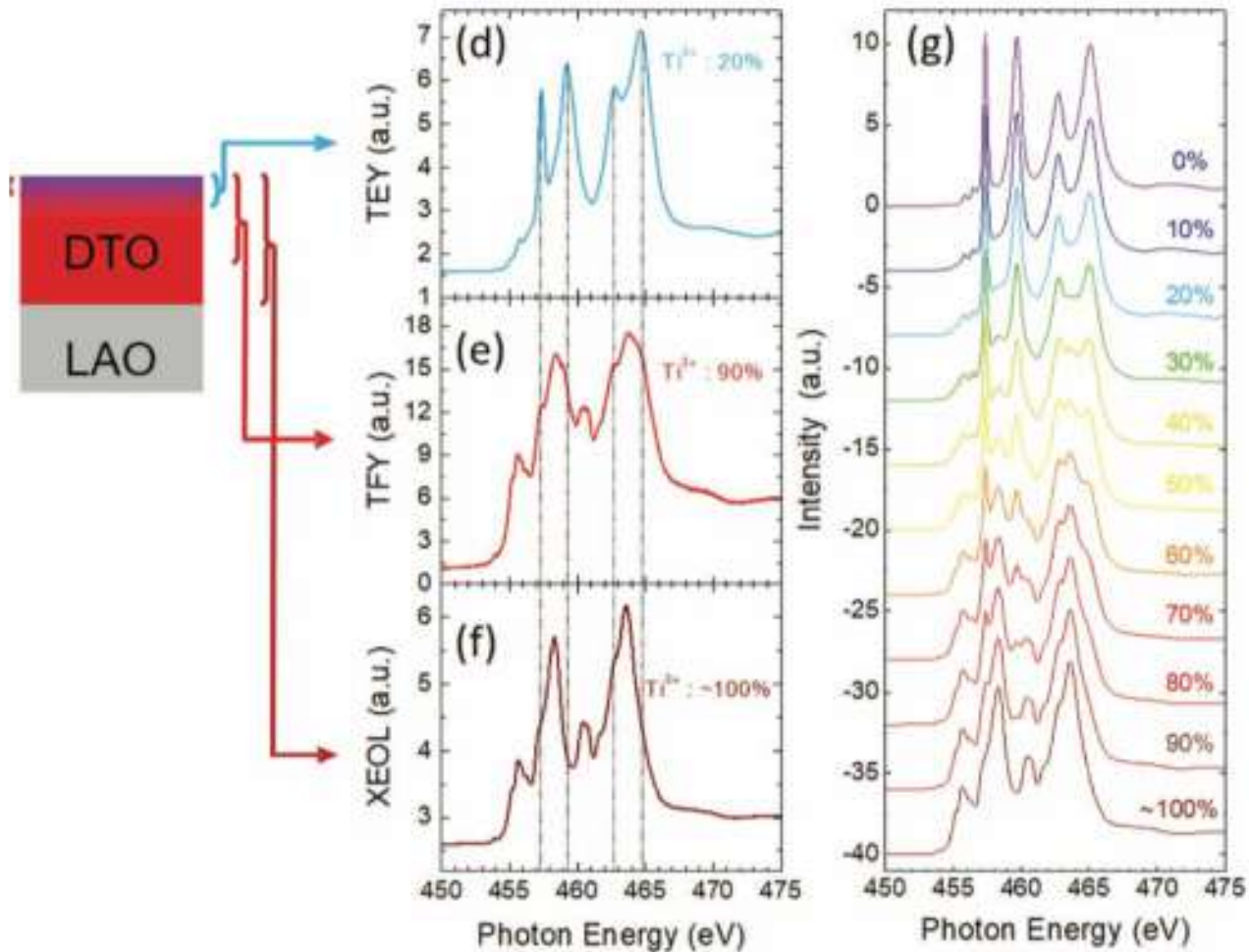
DTO

LAO



Example: A Living-Dead magnetic layer

A Living-Dead Magnetic Layer at the Surface of Ferrimagnetic DyTiO_3 Thin Films

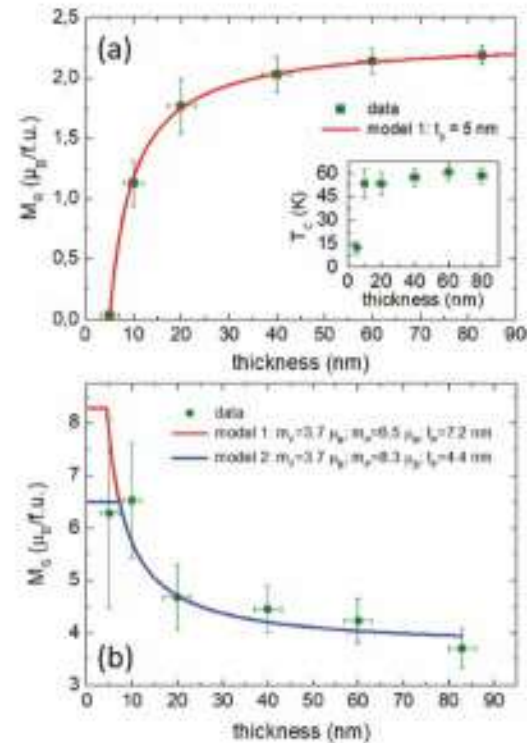
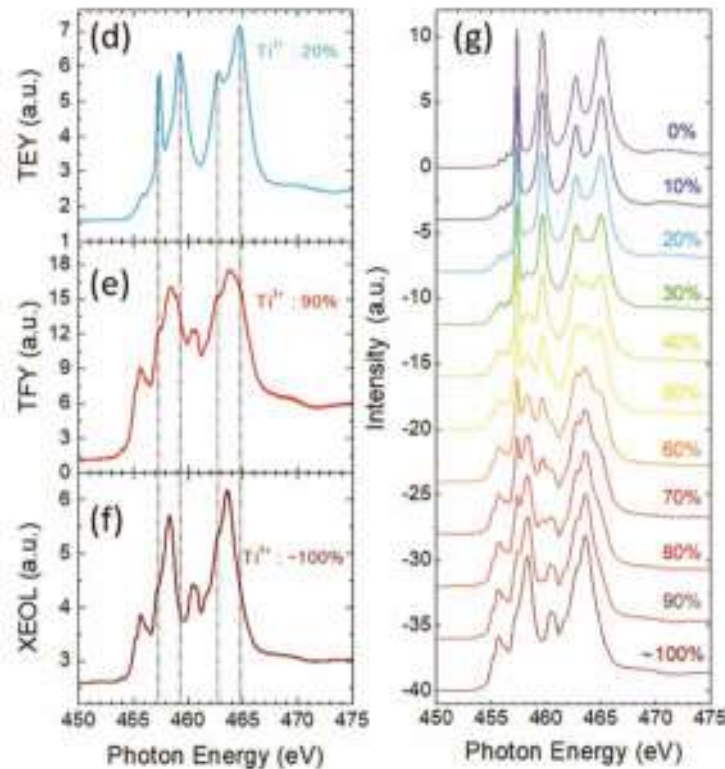


R. Aeschlimann, *et al*, *Adv. Mater.* **30**, 1707489 (2018).

Example: A Living-Dead magnetic layer

A Living-Dead Magnetic Layer at the Surface of Ferrimagnetic DyTiO₃ Thin Films

$$M_{\text{total}} = m_{\text{total}} \cdot t = m_{\text{P}} \cdot t_{\text{P}} + m_{\text{F}} \cdot t_{\text{F}}$$

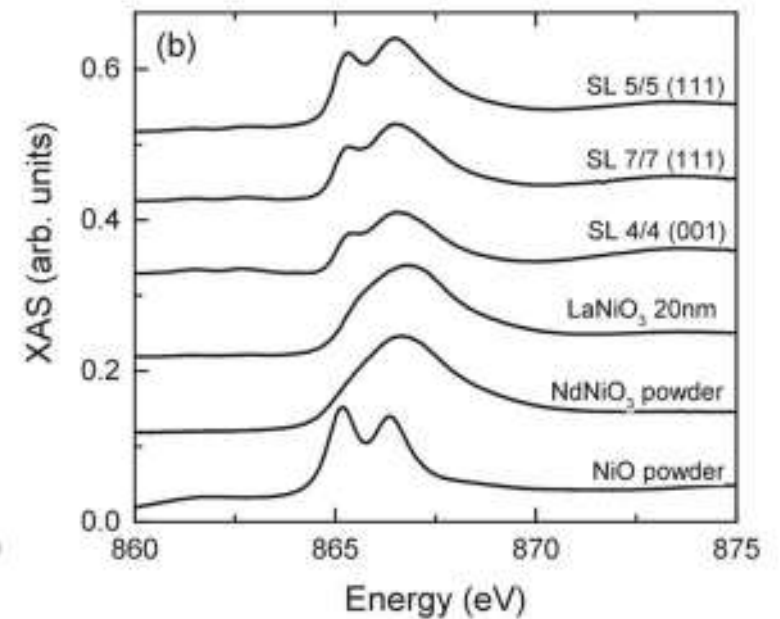
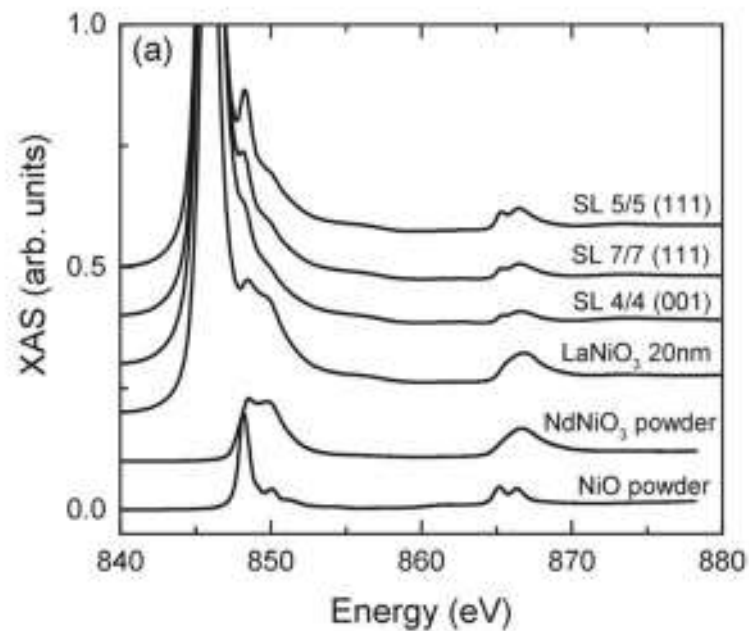
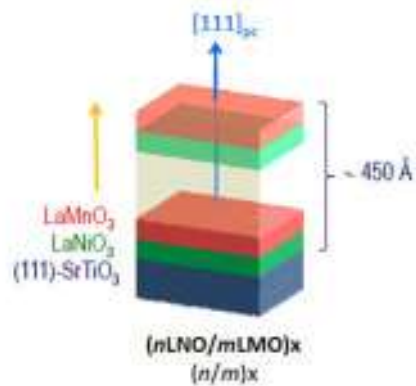


Example: charge transfer at LaMnO₃/LaNiO₃ superlattices

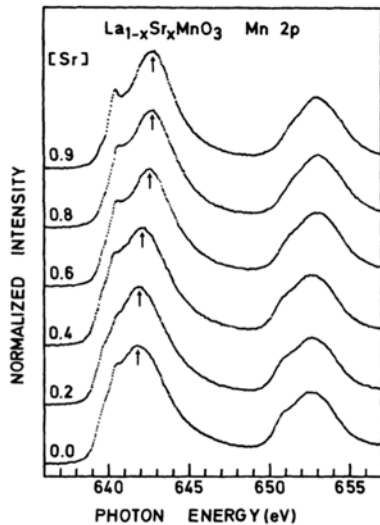
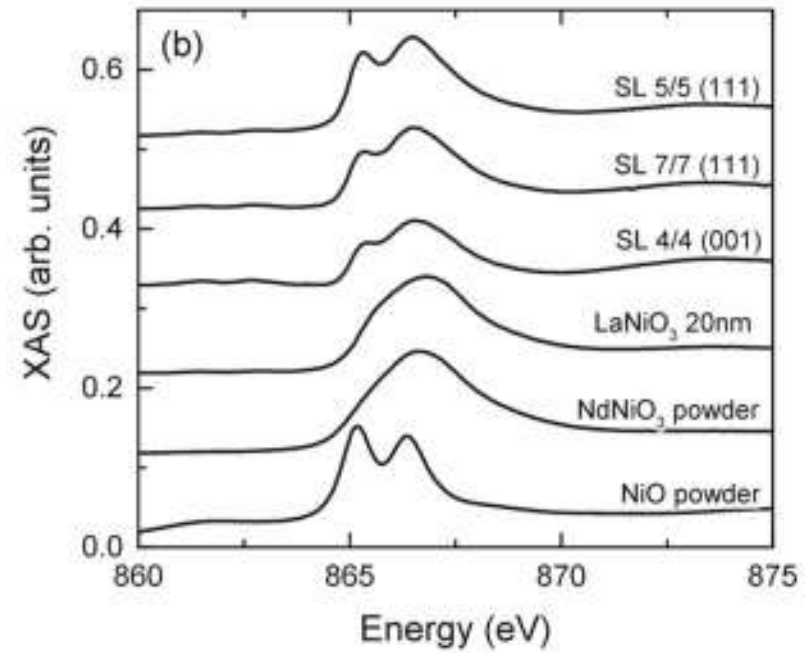
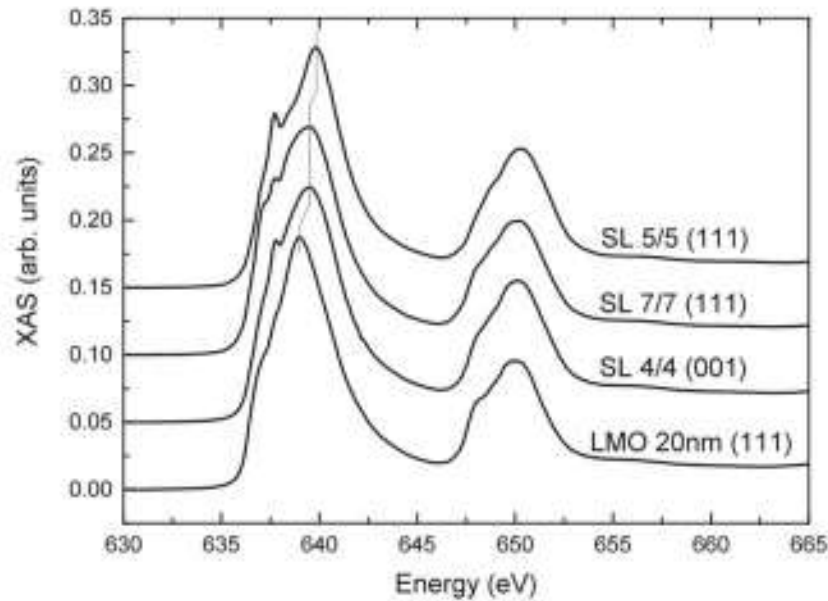
PHYSICAL REVIEW B **92**, 014426 (2015)

Interfacial properties of LaMnO₃/LaNiO₃ superlattices grown along (001) and (111) orientations

C. Piamonteze,¹ M. Gibert,² J. Heidler,¹ J. Dreiser,¹ S. Rusponi,³ H. Brune,³ J.-M. Triscone,² F. Nolting,¹ and U. Staub¹



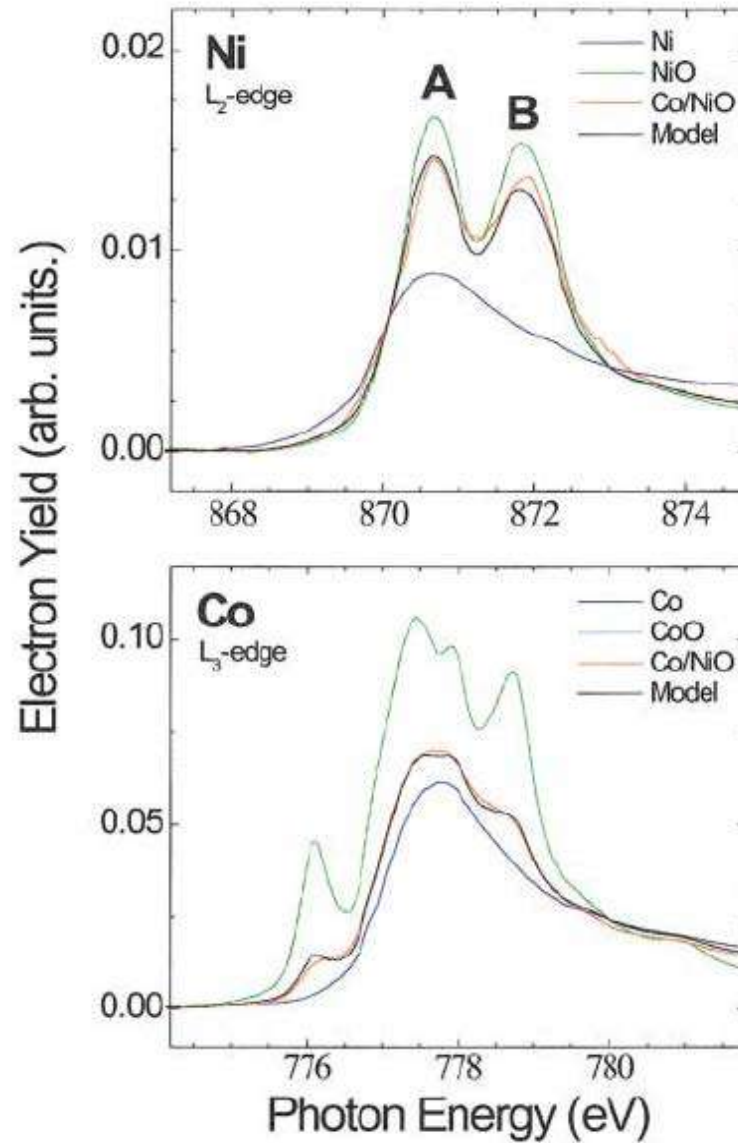
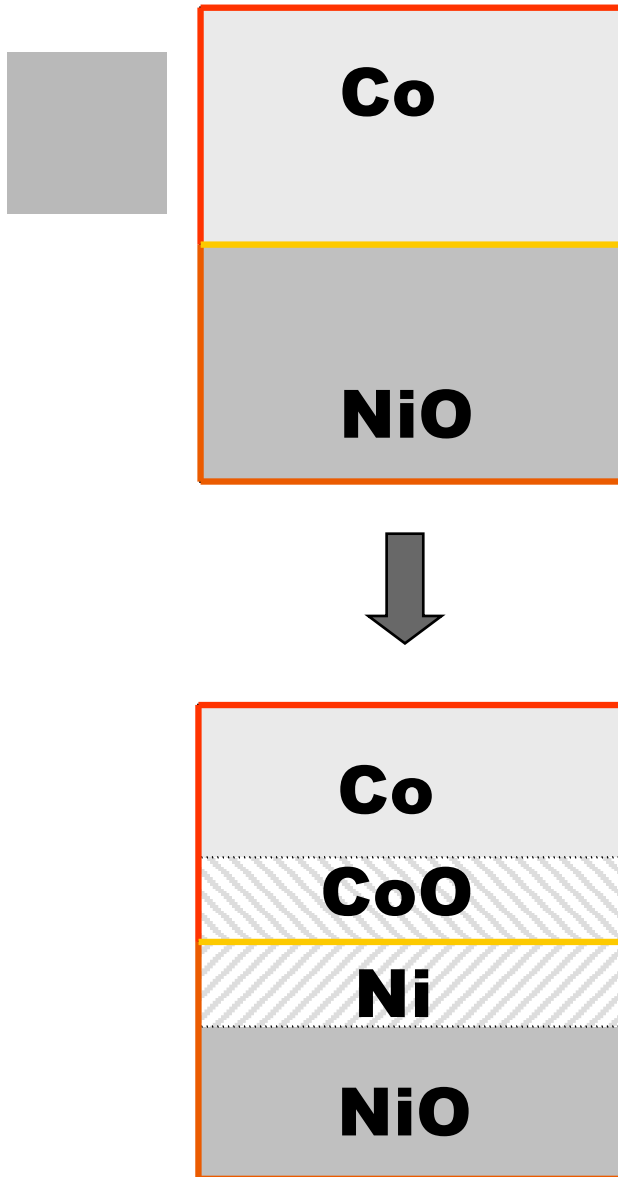
Example: charge transfer at LaMnO₃/LaNiO₃ superlattices



C. Piamonteze, *et al.*, PRB **92**, 014426 (2015).

M. Abbate, *et al.*, PRB **46**, 4511 (1992).

Example: Metal/oxide interface



Oxidation/reduction at the interface

Example: Metal/oxide interface TEY modeling

$$dN_{e,\text{Ni}} = I_0 e^{-z\mu_{\text{Ni}}(E)} \mu_{\text{Ni}}(E) G_{\text{Ni}}(E) e^{-z/\lambda_{\text{Ni}}} dz. \quad (\text{A1})$$

$$\begin{aligned}
 N_{e,\text{Ni}} + N_{e,\text{NiO}} = I_0 & \left(\frac{G_{\text{Ni}}(E)}{1 + \frac{1}{\mu_{\text{Ni}}(E) \lambda_{\text{Ni}}}} (1 - e^{-t_{\text{Ni}}[\mu_{\text{Ni}}(E) + 1/\lambda_{\text{Ni}}]}) \right. \\
 & + e^{-t_{\text{Ni}}[\mu_{\text{Ni}}(E) + 1/\lambda_{\text{Ni}}]} \frac{G_{\text{NiO}}(E)}{1 + \frac{1}{\mu_{\text{NiO}}(E) \lambda_{\text{NiO}}}} \\
 & \left. \times (1 - e^{-t_{\text{NiO}}[\mu_{\text{NiO}}(E) + 1/\lambda_{\text{NiO}}]}) \right). \quad (\text{A2})
 \end{aligned}$$

